APPLICATION OF CMAQ-APT TO CENTRAL CALIFORNIA

Submitted to

EPRI
3412 Hillview Avenue
Palo Alto, CA 94304

by

Krish Vijayaraghavan, Prakash Karamchandani,
and Christian Seigneur

Atmospheric & Environmental Research, Inc.
2682 Bishop Drive, Suite 120
San Ramon, CA 94583

September 2004
Document Number CP110-04-1

ACKNOWLEDGMENTS

We thank the California Air Resources Board for providing the CCOS emissions inventory and MM5 meteorology for the model simulations and surface air quality data for evaluating the models used in this work.

TABLE OF CONTENTS

LIST OF TABLES

LIST OF FIGURES

1. INTRODUCTION

Three-dimensional (3-D) models are frequently used to predict emission control impacts on concentrations of pollutants such as ozone and fine particulate matter ($PM_{2.5}$). Such models use a gridded representation of the atmosphere where atmospheric variables, such as chemical concentrations, are uniform within each grid cell. This approach averages emissions within the volume of the grid cell where they are released, and leads to significant errors for sources with spatial dimensions much smaller than that of the grid system. For example, stack plumes initially have dimensions of tens of meters, whereas the grid cell horizontal resolution is typically several kilometers in urban applications to about 100 km in regional applications. This artificial dilution of stack emissions leads to (1) unrealistic concentrations of emitted species near the stack, (2) incorrect chemical reaction rates due to the misrepresentation of the plume chemical concentrations and turbulent diffusion, and (3) incorrect representation of pollutant transport,

This limitation of 3-D grid models has been recognized for over two decades and various approaches have been taken to reduce the errors associated with the grid-averaging of stack emissions. The most common approach is the use of a Plume-in-Grid (PiG) treatment, i.e., a subgrid-scale representation of stack plumes imbedded in the 3-D model. The first subgrid-scale treatment of plumes in 3-D air quality models was developed by Seigneur et al. (1983). Other treatments of subgrid-scale effects have been developed over the years (e.g., Gillani, 1986; Sillman et al., 1990; Morris et al., 1991; Kumar and Russell, 1996; Myers et al., 1996; Gillani and Godowitch, 1999). All these models treat the plume at a subgrid-scale, thereby reducing some of the errors associated with the 3-D grid representation. However, they fail to represent the complex dispersion processes associated with the plume mixing into the background air because the plume dimensions are represented by simple geometric functions (columns, grids, ellipses, or Gaussian distributions). Physical phenomena such as the effect of wind shear on plume dispersion, the effect of plume overlaps (e.g., under conditions of reversal flow or merging of adjacent plumes), and the effect of atmospheric turbulence on chemical kinetics are not (or poorly) represented by such models.

Over the past few years, EPRI has sponsored the development of a new state-of-the-science PiG air quality model that can address the physical phenomena listed above explicitly, thereby providing a more realistic representation of the behavior of reactive plumes in the atmosphere. This PiG model consists of the reactive plume model, SCICHEM, imbedded into a three-dimensional grid-based model, the Community Multiscale Air Quality (CMAQ) modeling system. It is referred to as CMAQ with Advanced Plume Treatment (APT). An early version of CMAQ-APT was applied to explicitly simulate the plumes of two power plants for a five-day ozone episode in the Nashville/western Tennessee area (Karamchandani et al., 2000a). An improved version of the model was later used to explicitly simulate the plumes of the 30 largest NO_x point sources in the northeastern U.S. for a five-day episode in 1995 (Karamchandani et al., 2002).

In this report, we describe additional improvements to CMAQ-APT and the application of the model in California for an episode during the Central California Ozone Study (CCOS) in July/August 2000. CCOS is one of the components of the Central California Air Quality Studies (CCAQS) program. It consists of a field program (conducted during the summer of 2000), data analysis, emission inventory development, and modeling. CCOS was designed to characterize emissions, meteorology, and atmospheric processes affecting the production and fate of ozone in central California. The entire study is expected to be completed by 2005.

The California Air Resources Board (ARB) and local air quality management districts plan to use the CCOS results to prepare the demonstration of attainment for the ozone (O_3) standard for areas in central California that are currently in non-attainment. The primary modeling tool that is being used by the ARB, the air quality management districts, and their subcontractors is the Comprehensive Air Quality Model with extensions (CAMx). The study described in this report is designed to supplement the CAMx modeling results with those from an alternative modeling approach using CMAQ and CMAQ-APT and to understand the potential impacts of power plant NO_x emissions on O_3 formation in central California.

The report is organized as follows. Section 2 provides an overview of recent changes to CMAQ-APT, including the incorporation of a building downwash algorithm into the reactive plume model, as well as updates corresponding to the most recent versions of CMAQ and SCICHEM. Section 3 presents the application of CMAQ and CMAQ-APT to the CCOS domain. Model performance is evaluated in Section 4. Section 5 analyzes the impact of plume-in-grid modeling with CMAQ-APT, and Section 6 summarizes the results of the study.

2. IMPROVEMENTS TO CMAQ-APT

CMAQ-APT consists of the host 3-D air quality model, CMAQ, and the embedded reactive plume model, SCICHEM. A brief description is provided below. Additional details are provided in EPRI (2001) and Karamchandani et al. (2000a; 2002).

2.1. CMAQ-APT

CMAQ was developed by the U.S. Environmental Protection Agency (EPA) to address multiscale multi-pollutant air pollution problems (Byun and Ching, 1999). CMAQ treats the emissions, transport, dispersion, chemical transformations, gas-particle conversion and removal processes that govern the behavior of chemical pollutants in the atmosphere.

The reactive plume model used for the plume-in-grid treatment in CMAQ-APT is the Second-order Closure Integrated puff model (SCIPUFF) with CHEMistry (SCICHEM). Plume transport and dispersion are simulated with SCIPUFF, a model that uses a second-order closure approach to solve the turbulent diffusion equations (Sykes et al., 1988; 1993; Sykes and Henn, 1995). The plume is represented by a myriad of three-dimensional puffs that are advected and dispersed according to the local micrometeorological characteristics. Each puff has a Gaussian representation of the concentrations of emitted inert species. The overall plume, however, can have any spatial distribution of these concentrations, since it consists of a multitude of puffs that are independently affected by the transport and dispersion characteristics of the atmosphere. SCIPUFF can simulate the effect of wind shear since individual puffs will evolve according to their respective locations in an inhomogeneous velocity field. As puffs grow larger, they may encompass a volume that cannot be considered homogenous in terms of the meteorological variables. A puff splitting algorithm accounts for such conditions by dividing puffs that have become too large into a number of smaller puffs. Conversely, puffs may overlap significantly, thereby leading to an excessive computational burden. A puff merging algorithm allows individual puffs that are affected by the same (or very similar) micro-scale meteorology to combine into a single puff. Also, the effects of buoyancy on plume rise and initial dispersion are simulated by solving the conservation equations for mass, heat, and momentum.

The formulation of nonlinear chemical kinetics within the puff framework is described by Karamchandani et al. (2000b). Chemical species concentrations in the puffs are treated as perturbations from the background concentrations. The chemical reactions within the puffs are simulated using a general framework that allows any chemical kinetic mechanism to be treated.

In the following sections, we provide a brief description of recent changes to SCICHEM and CMAQ-APT since the last application of CMAQ-APT to the northeastern United States by Karamchandani et al. (2002). These changes include both the incorporation of a treatment for the effects of building downwash in SCICHEM and CMAQ-APT as part of the study described here, as well as changes that were necessitated by other updates to CMAQ (as part of ongoing CMAQ development at EPA) and SCICHEM (as part of ongoing SCICHEM improvement for various projects).

2.2. SCICHEM-PRIME

As part of the study described here, SCICHEM was modified to incorporate a state-of-the-science module for treating the effects of building downwash on plume rise and dispersion of stack emissions. The building downwash treatment is based on the Plume Rise Model Enhancements (PRIME) model (Schulman et al., 2000). PRIME incorporates the two fundamental features associated with building downwash: enhanced plume dispersion coefficients due to the turbulent wake, and reduced plume rise caused by a combination of the descending streamlines into the lee of the building and the increased entrainment in the wake. PRIME has been incorporated into the U.S. EPA regulatory model, ISC3. It has been tested against data from field studies and wind tunnels.

The PRIME model was incorporated into SCICHEM by scientists at Titan/ARAP. The PRIME calculations are activated whenever building data are provided for a particular stack. PRIME is then used to describe the plume to a point beyond the building wakes and where the plume has achieved final rise. At this point, a SCICHEM source is then initialized with the appropriate size and emissions.

This version of SCICHEM, referred to as SCICHEM-PRIME, was used by AER to simulate plumes from the Pittsburg power plant in the Sacramento River delta and the Moss Landing power plant on the Pacific Coast near Monterey during July and August 2000 as part of a separate but related EPRI-sponsored study (EPRI, 2003a). The model results were compared with aircraft measurements of these plumes conducted by the Tennessee Valley Authority (TVA) during the same period as part of CCOS. Background concentrations for SCICHEM-PRIME were obtained from a CMAQ simulation of the same period.

2.3. Updates to SCICHEM-PRIME and CMAQ-APT

The version of CMAQ-APT used by Karamchandani et al. (2002) in their PiG application for the northeastern United States was based on the August 2000 version of CMAQ and SCICHEM Version 1302. SCICHEM-PRIME (Version 1402), described in Section 2.2, was also embedded into the August 2000 version of CMAQ during the early part of this study in January 2002. This version of CMAQ-APT was tested briefly for a hypothetical source using CMAQ data files for the Nashville/western Tennessee area. However, at EPRI's request, further work on this project (including detailed testing of the implementation) was postponed until the beta-testing of SCICHEM-PRIME and CMAQ-APT and further improvements to SCICHEM-PRIME following the beta-testing were completed (under separate EPRI projects), and also until final data files were available from the California ARB for the CCOS episode that would be simulated in this project.

The beta-testing of SCICHEM-PRIME and CMAQ-APT was completed in late 2002 in a separate EPRI-sponsored study (EPRI, 2003b). The results of the beta-testing were used to make additional modifications to SCICHEM in another EPRI-sponsored project conducted by scientists at Titan/ARAP, resulting in a significantly revised version of SCICHEM-PRIME (Version 1600) that was made available to AER in late 2003. In the meantime, there were several updates to CMAQ (four public releases of CMAQ after the August 2000 release).

To ensure that the version of CMAQ-APT used in the current study was up-to-date, we used the latest available versions of CMAQ and SCICHEM. The latest publicly available

version of CMAQ is the September 2003 release (Version 4.3), while the latest available version of SCICHEM-PRIME is Version 1601 (January 2004 release). These versions of CMAQ and SCICHEM-PRIME are significantly different from those used in the previous implementation of CMAQ-APT (August 2000 and Version 1402, respectively). In particular, there are significant structural changes to CMAQ that are directly relevant to the SCICHEM implementation, primarily the Fortran 90 updates and the introduction of dynamic arrays. Thus, considerable effort was expended in updating CMAQ-APT to the latest versions of CMAQ and SCICHEM-PRIME.

In addition to these model updates, we implemented the Young & Boris chemistry solver (Young and Boris, 1977), used in SCICHEM-PRIME, in the September 2003 release of CMAQ. This was done to ensure that the same chemical solver would be used in the host model and the embedded reactive plume model for both the base case (i.e., without plume-in-grid) and plume-in-grid simulations. As described in Sections 3.2 and 3.5, we tested this modification for the CCOS domain by comparing the results from a base case CMAQ simulation using the Young & Boris solver with those from a base case simulation using the default CMAQ chemistry solver, the Euler Backward Iterative (EBI) method.

3. MODEL APPLICATION TO THE CCOS DOMAIN

3.1. Episode Characterization

CMAQ and CMAQ-APT were applied for the July/August 2000 CCOS episode. The characteristics and evolution of this episode have been discussed at length by Lehrman et al. (2004) and the California Air Resources Board (ARB, 2004). The ozone episode covered a five-day period from 29 July to 2 August, 2000. The major findings on meteorology and air quality during the episode are reproduced below.

A typical Great Basin high pressure system was observed during the course of this episode (ARB, 2004). Prevailing winds were characterized by persistent inflow to the Central Valley from the central coast through the Carquinez Strait, passes and lower gaps in the coastal ranges. Peak inflow occurred in the afternoon and minimum inflow in the predawn hours.

The diurnal cycle on July 29 and July 30 was characterized by a valley-wide nocturnal jet in the San Joaquin Valley (SJV) followed at daybreak by a cyclonic eddy in the central SJV (Lehrman et al., 2004). Afternoons were dominated by valley-wide upvalley winds; southeasterly in the Sacramento Valley (SacV) and northwesterly in the SJV. The nocturnal jet on the evening of July 31 began to develop in the northern SJV but was absent in the central and southern SJV. A transient low-level perturbation moved from south to north in the early morning of August 1, resulting in widespread southerly winds in the central and southern SJV. By noon on August 1, a strong onshore flow developed producing general northwesterly low-level winds throughout the SJV that became quite strong in the evening. An unorganized light wind field developed in the SJV during the morning of August 2. A vigorous onshore flow again developed in the afternoon of August 2 producing uniformly strong northwesterly winds in the northern SJV, light upvalley winds in the central SJV, and southeasterly winds in the southern SJV. Clouds reduced insolation in the SJV during the episode, reaching a minimum on July 31, thereby possibly impacting the extent of photochemistry.

Table 3-1 summarizes the peak one-hour ozone concentrations measured in the extended CCOS network from July 30 to August 1, 2000 (ARB, 2004). This time period corresponds to the duration of model analysis in this work. Peak ozone values on July 30 occurred at Santa Clarita and in the San Joaquin Valley, where values near 130 ppb were recorded at Parlier and Edison; the Bay Area and Sacramento region experienced no federal 1-hour exceedances that day. On July 31, peak network ozone levels (120 ppb range) were measured at Livermore, Patterson Pass, and in the Sierra foothills east of Fresno. Livermore experienced the only exceedance of the federal 1-hour ozone standard on that day in the CCOS domain. On August 1, peak ozone levels were experienced along the Sierra foothills from Sloughhouse to the San Andreas-Sonora area, and Kings Canyon. The only federal 1-hour exceedances on that day occurred in the Sacramento region, with the San Andreas station recording a peak value of 134 ppb.

Table 3-1. Measured peak 1-hour ozone concentrations (ppb) in the CCOS network from July 30 to August 1, 2000 (after ARB, 2004) [a].

Date	**Domain-wide**	**Sacramento Non-attainment area**	**Bay Area**	**San Joaquin Valley North**	**San Joaquin Valley South**
July 30, 2000	Santa Clarita (SCFS) 131	Sloughhouse (SLU) 121	Livermore (LVF) 82	Parlier (PLR) 129	Edison (EDS) 128
July 31, 2000	Livermore (LVF) 126	Davis (DVS) 103	Livermore (LVF) 126	Clovis (CLO) 118	Edison (EDS) 115
August 1, 2000	San Andreas Stn (SGS) 134	San Andreas Stn (SGS) 134	Livermore (LVR1) 94	Fresno Sierra Skypark (FSS) 118	Arvin (ARV) 116

(a) Station ID provided in parentheses

There were several large wildfires in California during the July/August CCOS episode, and some of the peak ozone measurements during the episode may have been influenced in part by wildfire emissions (ARB, 2004). The largest wildfires occurred in eastern Tulare County on July 29 and 30, 2000.

3.2. Model Configuration

The version of CMAQ released by the U.S. Environmental Protection Agency (EPA) in September 2003 (Version 4.3) was used in this study. CMAQ offers several options for some science modules. The options selected for model simulations in this work are summarized in Table 3-2. The plume-in-grid option shown was used in the CMAQ-APT simulation. As discussed in Section 2, SCICHEM is the reactive plume component of CMAQ-APT. The interface between SCICHEM and CMAQ has been described in detail in EPRI (2001) and Karamchandani et al. (2002). This interface is implemented via the PING_APT module in CMAQ-APT.

As discussed in Section 2 and in EPRI (2001), the Young & Boris (YB) solver was used for the numerical solution of gas-phase chemical kinetics in the CMAQ and CMAQ-APT simulations. A reference CMAQ simulation was also conducted using the Euler Backward Iterative (EBI) method, the default gas-phase chemistry solver in CMAQ, to verify that the YB solver was correctly implemented in CMAQ. The two CMAQ simulations with the YB and EBI solvers are discussed further in Section 3.5.

3.3. Modeling Domain and Grid System

The CCOS air quality modeling domain for this study was based on the grid definition in the CAMx input files (subsequently used to create CMAQ model inputs) provided by the ARB. The modeling domain for CMAQ and CMAQ-APT extends from Santa Barbara County in the south to Shasta County in the north, and from the Pacific Ocean into Nevada in the east (see Figure 3-1a). A map of California counties in the study area is presented in Figure 3-1b. The domain is defined in a Lambert Conical Projection with reference latitudes at 30 and 60 N, the central meridian at 120.5 W, and the coordinate system origin at 120.5 W and 37 N. The southwest corner of the grid is 376 km west of and 292 km south of the coordinate system origin.

Table 3-2. CMAQ configuration options selected for the CCOS simulations.

Science Module	Options Selected
Horizontal and vertical advection	Piecewise parabolic method (PPM)
Gas-phase chemistry	Carbon Bond Mechanism (CBM-IV)
Numerical solver for chemical kinetics	Young & Boris (YB) solver [(a)] Euler Backward Iterative (EBI) solver [(b)]
Horizontal diffusion	K theory with constant eddy diffusivity (multiscale module)
Vertical diffusion	K theory (eddy module)
Plume-in-grid	PING_APT[(a), (c)]

(a) this work only; not available in the standard CMAQ release from EPA

(b) used in a test CMAQ simulation for comparison with the Young & Boris solver

(c) used for the CMAQ-APT application

Figure 3-1a. Modeling domain for the CCOS simulations.

Figure 3-1b. Map of California counties in the study area.

The horizontal study domain is comprised of 185 x 185 grid cells with a resolution of 4 km, while the vertical grid structure consists of 20 layers from the surface to the tropopause with finer resolution near the surface (e.g., the surface layer is 30 m deep). Table 3-3 lists the sigma coordinates of the grid layers and their approximate heights in meters above ground level (m agl).

3.4. Preparation of Inputs

The meteorological fields are from a prognostic simulation conducted with the non-hydrostatic meteorological model, MM5, using four-dimensional data assimilation (FDDA). The emissions, initial conditions and boundary conditions were available from an air quality simulation conducted with another air quality model (CAMx). The MM5 meteorology and CAMx emissions, initial and boundary condition files for the CCOS modeling period (July 29 to August 2, 2000) were provided by the ARB. These files were converted to CMAQ model-ready input. The modeling period for the CMAQ application was chosen to be from 12 GMT on July 29, 2000 to 12 GMT on August 2, 2000, based on the availability of input data.

Meteorological files for CMAQ were created from the CCOS MM5 file using the MCIP (Version 2.2) processor. Initial condition (IC) and boundary condition (BC) files for CMAQ were developed with the same concentration profiles as in the CAMx IC and BC files using modified forms of the CMAQ ICON and BCON processors. Daily photolysis files for July 29 through August 2, 2000 were created using the CMAQ JPROC processor with TOMS ozone column data as input.

The daily CAMx point source emission files were converted to 3-D gridded CMAQ files using the plume rise processor in SMOKE. The daily CAMx area source files were converted to 2-D gridded CMAQ files. The 2-D and 3-D gridded CMAQ files were merged to construct CMAQ-ready 3-D emission files. Two other emission files were developed for the CMAQ-APT and background simulations discussed later in Sections 3.6 and 3.7. The first contained emissions from the point sources selected for plume-in-grid treatment and was in SCICHEM format. The second included emissions from all other sources and was in the standard CMAQ format. Both emission files were used in

the CMAQ-APT simulation. Section 3.6 provides details on the selection of point sources that were included in the first file. In the background simulation, only the second file was used.

Table 3-3. CMAQ grid layers for the CCOS simulations.

Layer Number	σ-p	Approximate layer top (m agl)
20	0.0000	14000
19	0.1120	10500
18	0.1917	8832
17	0.3536	6213
16	0.4954	4440
15	0.6254	3078
14	0.7301	2111
13	0.8107	1430
12	0.8431	1170
11	0.8709	952
10	0.8946	770
9	0.9148	617
8	0.9319	490
7	0.9463	385
6	0.9585	296
5	0.9688	222
4	0.9774	160
3	0.9846	109
2	0.9907	66
1	0.9958	30
0	1.0000	0

3.5. CMAQ Base Simulation

Two CMAQ simulations, one each with the YB and EBI gas-phase chemistry solvers, were conducted over the modeling domain using the inputs described above. The simulations were performed for the 4-day period from 12 GMT on July 29, 2000 to 12 GMT on August 2, 2000. The first 19 hours of the simulation were used to spin-up the model; hence, the study period begins at 7 GMT, i.e. 0 PDT, on July 30, 2000.

The CMAQ simulation conducted with the YB chemical kinetics solver is the base case application for this study. As discussed earlier, use of the YB solver in both CMAQ and SCICHEM ensures consistency between the host and plume models. The purpose of conducting the EBI simulation was to verify that there were negligible differences in concentration fields between using the EBI solver, the default scheme in CMAQ, and the YB solver. The computational processing (CPU) time for the CCOS simulation using the YB solver was about a factor of two higher than that using the EBI solver. Implementation of the latter solver in SCICHEM would permit its use in CMAQ and CMAQ-APT, potentially halving computational time.

An examination of model output from the simulations employing the EBI and YB solvers showed that the predicted concentrations from the two simulations were comparable. Figure 3-2 presents surface O_3 concentrations at the time of peak O_3 prediction obtained by both solvers. The spatial patterns in O_3 concentrations are very similar. Both numerical methods simulate nearly identical maximum O_3 concentrations (228 and 229 ppb) and at the same time (4 p.m. PDT on July 30, 2000) and location (southeastern Tulare County) during the episode. The O_3 peaks are due to the occurrence of large wildfires in eastern Tulare County near the Sierra Nevada. Figure 3-3, depicting total hourly nitrogen oxides (NO_x) emissions, shows the presence of very high emissions from wildfires in that part of the domain. The emissions of high levels of NO_x and hydrocarbons from the wildfires result in excessive O_3 concentrations in that region.

(a)

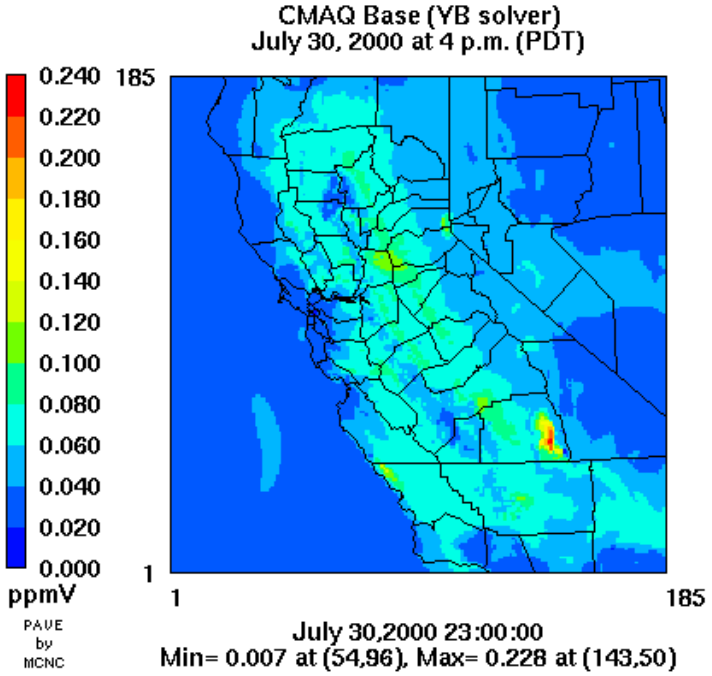

(b)

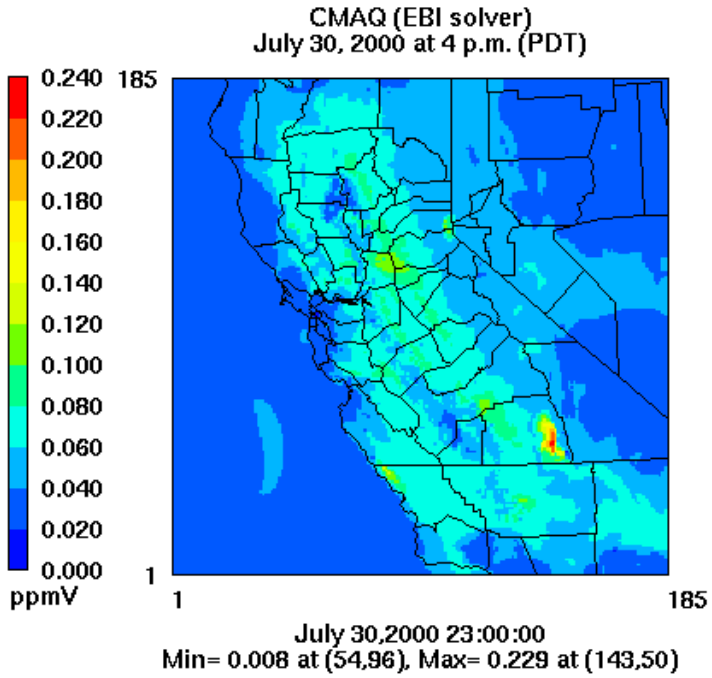

Figure 3-2. Surface O_3 concentrations simulated by CMAQ with the (a) YB and (b) EBI chemistry solvers at 4 p.m. PDT on July 30, 2000.

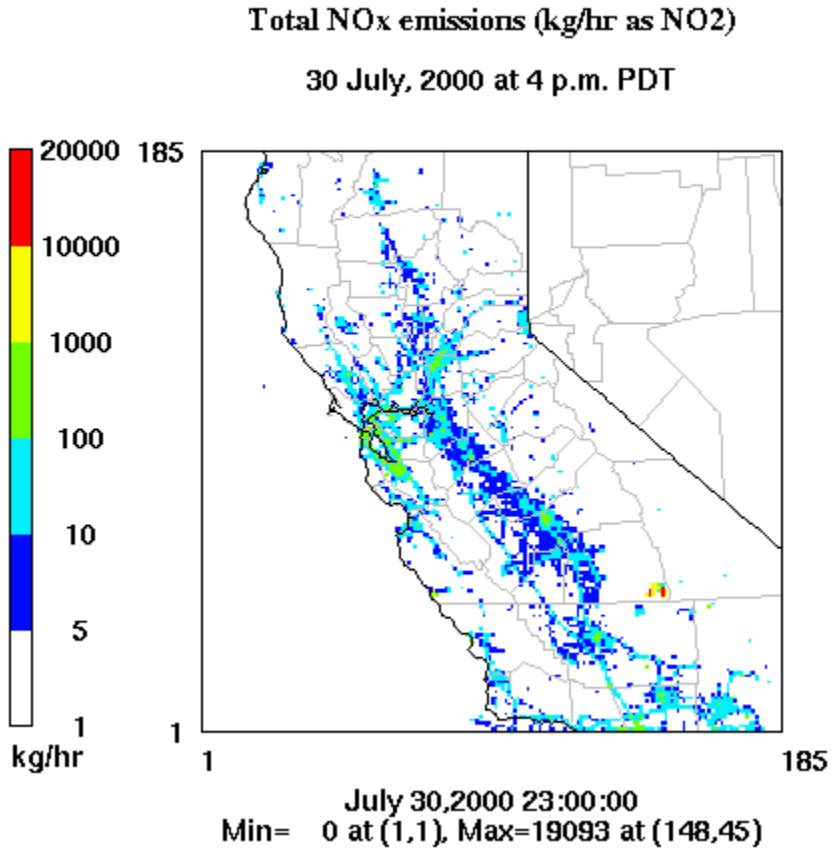

Figure 3-3. Total NO_x emissions (kg/hr as NO_2) at 4 p.m. PDT on July 30, 2000.

Figure 3-4 presents a time series of differences in domain-wide average surface ozone concentrations simulated by CMAQ using YB and EBI over the study period. The differences in results from the two solvers are negligible (less than 0.3 ppb). A similar trend is shown in Figure 3-5 for HNO_3 predictions with the two solvers, with differences less than 0.01 ppb.

All subsequent references to the CMAQ "base" simulation in the remainder of this report will denote the CMAQ simulation with the YB solver.

Figures 3-6, 3-7, and 3-8 present the spatial patterns of surface ozone concentrations simulated in the CMAQ base case at 3 p.m. PDT on 30 and 31 July, 2000 and at 4 p.m. PDT on 1 August, 2000, respectively. These times correspond to the hours of maximum ozone impact due to the emission sources of interest in this study. The selection of these sources and the choice of the times are discussed in detail in Sections 3.6 and 4, respectively.

Figure 3-6 depicts the distribution of ozone simulated in the surface layer at 3 p.m. PDT on July 30 in (a) the entire domain and (b) a small sub-domain covering the extended San Francisco Bay Area. As discussed earlier, the peak O_3 concentration of 222 ppb in eastern Tulare County is, in part, due to wildfires in that region. Other exceedances of the federal 1-hour ozone standard are simulated near Bakersfield, Fresno, San Simeon (San Luis Obispo County), and the Sacramento metropolitan area. In these regions, modeled ozone levels are in the 120 ppb range. Simulated O_3 exceeds 70 ppb along most of the western and eastern edges of the Central Valley. In the immediate vicinity of San Francisco Bay, ozone levels are mostly near background values. Ozone concentrations higher than 90 ppb are estimated at the border of Santa Clara/Merced Counties and in Modesto, Turlock, and Manteca along Highway 99. O_3 concentrations elsewhere inland are mostly in the 60 to 80 ppb range.

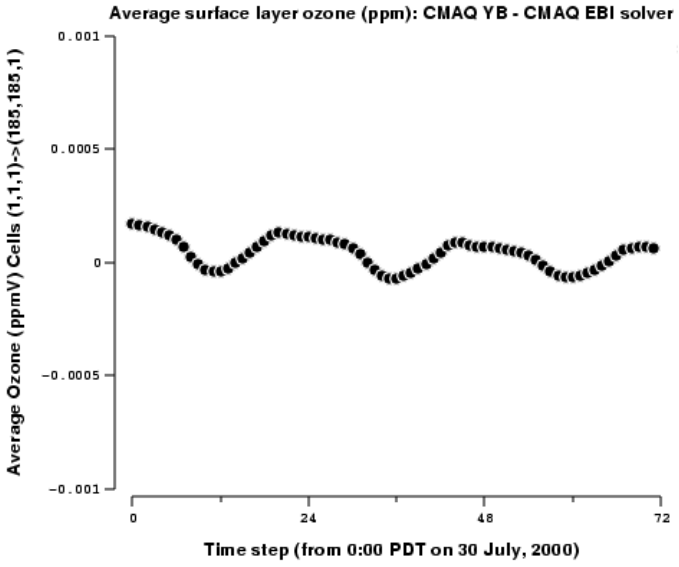

Figure 3-4. Time series of differences in average surface O_3 concentrations (ppm) simulated by CMAQ YB and CMAQ EBI.

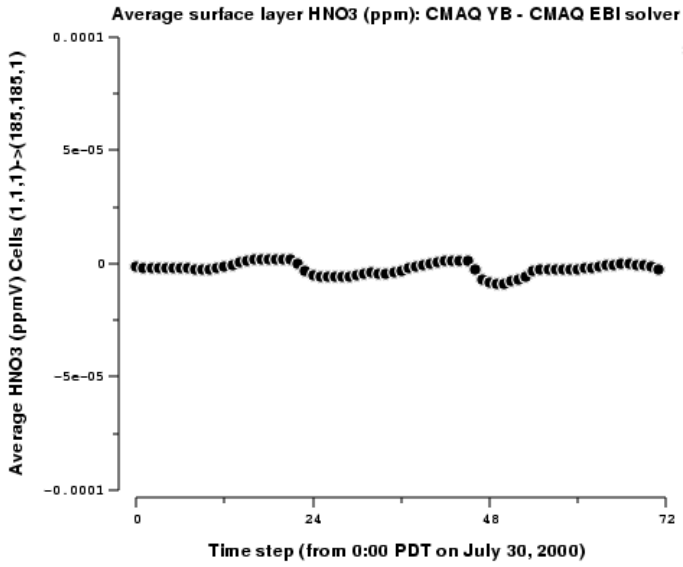

Figure 3-5. Time series of differences in average surface HNO_3 concentrations (ppm) simulated by CMAQ YB and CMAQ EBI.

(a)

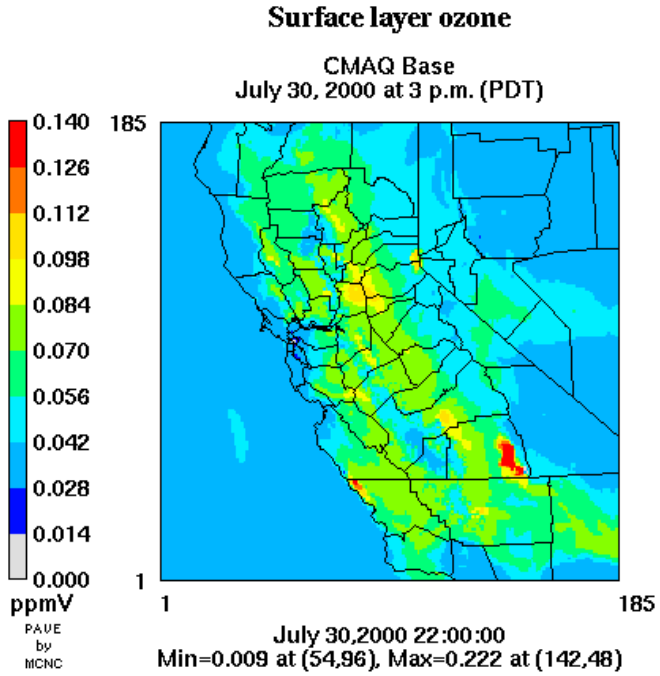

(b)

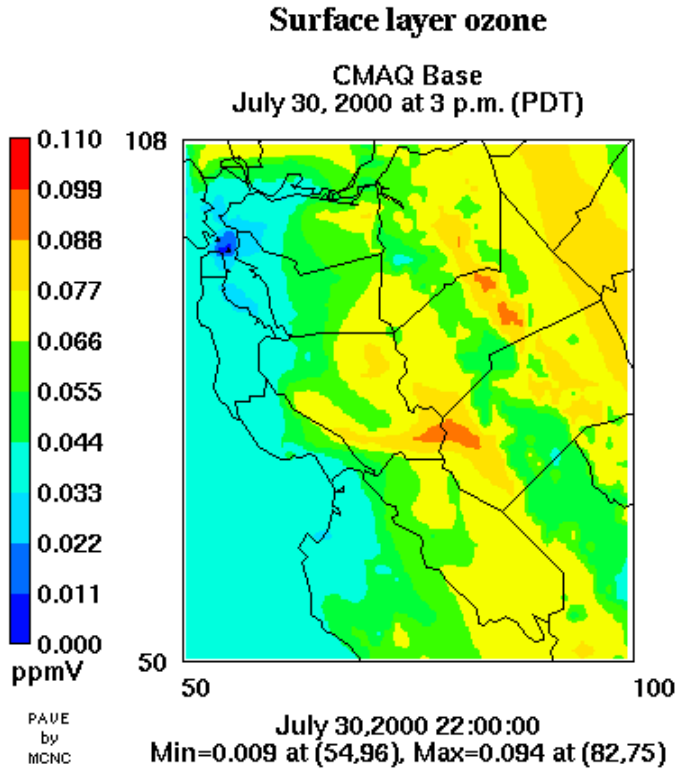

Figure 3-6. Surface O_3 concentrations simulated by CMAQ at 3 p.m. PDT on July 30, 2000 in (a) the entire domain and (b) the extended Bay Area.

(a)

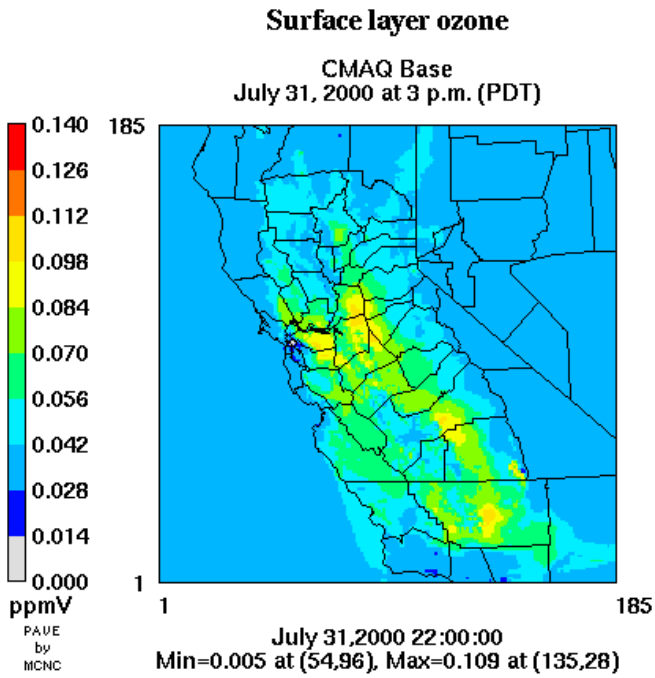

(b)

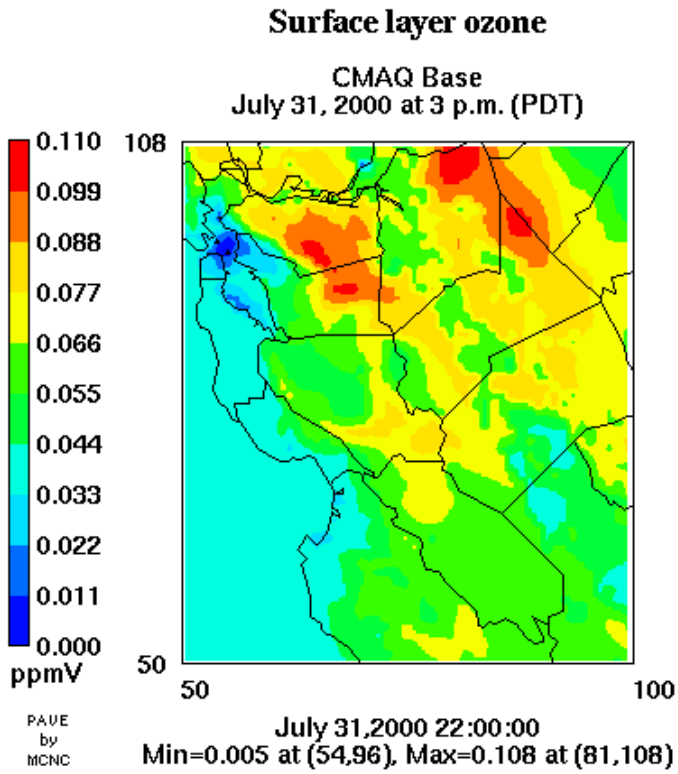

Figure 3-7. Surface O_3 concentrations simulated by CMAQ at 3 p.m. PDT on July 31, 2000 in (a) the entire domain and (b) the extended Bay Area.

(a)

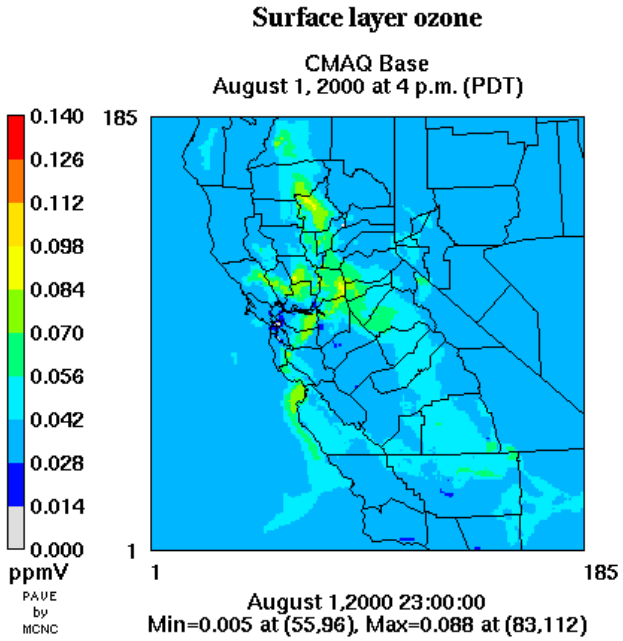

(b)

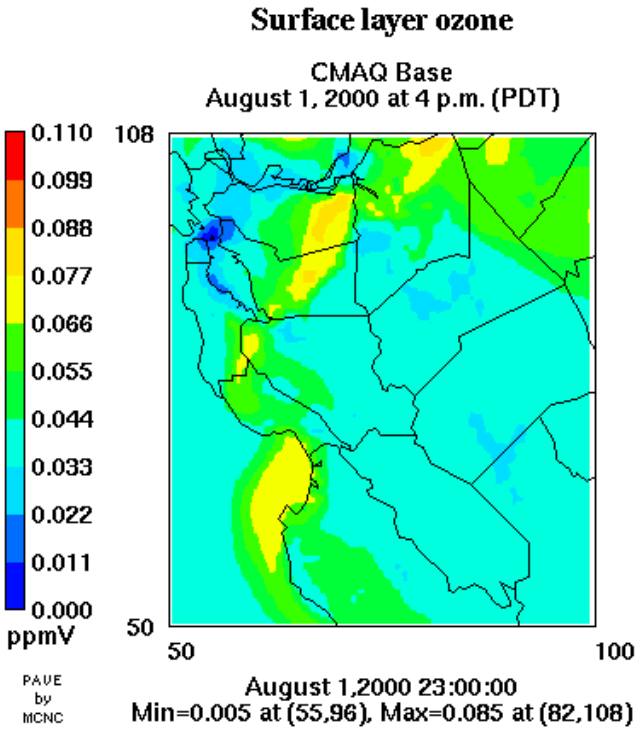

Figure 3-8. Surface O_3 concentrations simulated by CMAQ at 4 p.m. PDT on August 1, 2000 in (a) the entire domain and (b) the extended Bay area.

The calculated peak ozone concentration of 109 ppb at 3 p.m. PDT on July 31, 2000 is simulated near Bakersfield and Edison. This value agrees well with the measured ozone level of 115 ppb at Edison on that day (see Table 3-1). Ozone concentrations in the 80 to 100 ppb range are simulated in parts of Contra Costa and Alameda Counties (including Livermore), and east of the Sacramento-San Joaquin Delta. Simulated ozone concentrations decline on August 1, 2000 with a peak value of only 88 ppb. Ozone levels above 80 ppb are seen in parts of the Sacramento Valley along the Sierra Nevada, in Monterey Bay, and in eastern Contra Costa and Alameda Counties. We present a detailed performance evaluation of the model with observations in Section 4.

HNO_3 concentrations simulated by CMAQ are discussed in Section 5 in the context of the plume-in-grid modeling.

3.6. CMAQ-APT Simulation

Fifty-six (56) stacks from the ten plants that had the highest NO_x emission rates in the modeling domain were selected for explicit plume treatment in the CMAQ-APT simulation. Stacks with NO_x emissions less than 1% of those from the top stack emitter in each of the ten plants were retained for standard (i.e., gridded) CMAQ modeling. Emissions from wildfires and other sources in the domain were also retained in the gridded inventory. Some of the 56 stacks selected for plume modeling were located in close proximity of each other and had similar heights. These stacks were combined into single sources, each with an effective stack diameter, height, flue gas temperature, and flue gas velocity based on the principles of conservation of flow, momentum and buoyancy. This procedure was adopted to avoid significant computational delays in processing puffs that are very near each other and also to reduce the total number of point sources that were explicitly treated with the plume model. Overall, 14 effective stacks were used for plume modeling. The names of the 10 plants were determined using information in the UAM pre-processor emissions files provided by the ARB.

The ten plants selected and their daily NO_x emission rates are shown in Table 3-4. Figure 3-9 shows the location of these sources (some of these sources are aggregates of stacks in the same grid cell). Also shown is the NO_x-emitting rank of each plant. The Pittsburg

power plant and the Riverside Cement plant have the highest NO_x emissions in the CCOS domain. The ten plants selected for PiG treatment represent about 4% of the total NO_x emission inventory over the modeling domain.

Table 3-4. Plants with the top ten NO_x emission rates in the modeling domain.

Rank	Plant Name	Number of original stacks	Number of effective stacks	NO_x emissions (Mg/day as NO_2)
1	Pittsburg Power Plant	7	2	15.5
2	Riverside Cement Co.	8	1	14.8
3	CEMEX: California Cement	2	1	13.2
4	Moss Landing Power Plant	2	1	13.1
5	Martinez Refining Co.	20	3	8.8
6	Hanson Permanente Cement	1	1	8.8
7	Unknown	3	1	8.3
8	Portland Cement Co.	1	1	6.6
9	IMC Chemicals	10	2	6.2
10	Contra Costa Power Plant	2	1	5.8
	Total	**56**	**14**	**101.2**

A CMAQ-APT simulation was conducted over the CCOS domain for the 4-day period from 12 GMT on July 29, 2000 to 12 GMT on August 2, 2000. This simulation was conducted without the building downwash (PRIME) option, since a previous modeling study with SCICHEM (Karamchandani and Vijayaraghavan, 2001) had shown negligible effects of building downwash for the Pittsburg and Moss Landing power plants. These two plants have some of the tallest stacks among the ten plants selected for PiG modeling in the study described in this report. This decision was made in consultation with EPRI, ARB and CEC scientists in a joint conference call on April 19, 2004. The impacts of PiG modeling are discussed in Section 5.

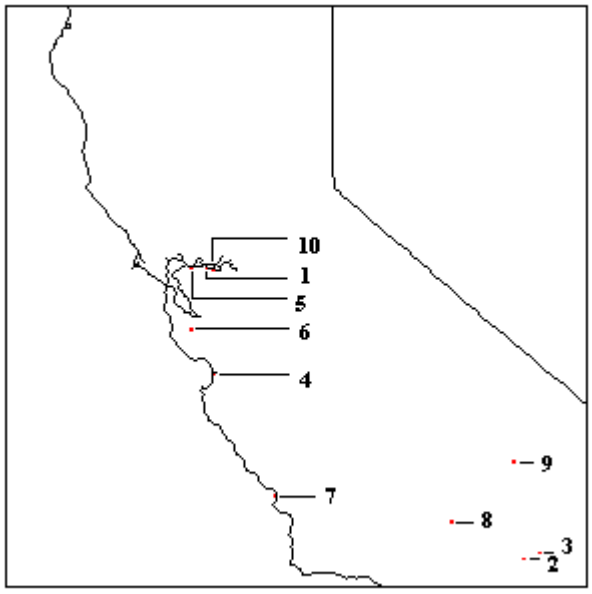

Figure 3-9. Locations of the ten plants simulated with an explicit plume-in-grid treatment. The number next to each plant indicates its NO_x emissions rank.

3.7. CMAQ Background Simulation

To better understand the effect of using a plume-in-grid treatment, we conducted another simulation for the CCOS modeling domain with CMAQ without the emissions from the ten largest NO_x emitting plants selected for plume-in-grid treatment. The concentrations from this simulation can be considered to be "background" values for these point sources. Relative to the results from this "background" simulation, the CMAQ-APT simulation and the CMAQ base simulation will show the effect of the NO_x emissions from these point sources with and without PiG treatment, respectively. In other words, we can get a measure of the ozone and nitric acid that can be produced (or titrated, in the case of O_3) in the plumes of these point sources with and without PiG treatment, particularly for isolated sources.

4. MODEL PERFORMANCE EVALUATION

In this section, we present the model performance evaluation results for both the base (CMAQ) and plume-in-grid (CMAQ-APT) simulations using hourly surface observations of O_3, NO_x, NO_y and CO at monitoring locations in the CCOS network. These observations were obtained from the ARB (Jackson, 2004). The model evaluation results are presented in the form of graphical displays as well as statistical metrics.

4.1. Graphical Evaluation

Figures 4-1 through 4-4 compare the time series of surface ozone concentrations estimated in the CMAQ-Base and CMAQ-APT simulations with the corresponding observations at four monitoring locations in the CCOS network: San Andreas Station (SGS), Parlier (PLR), Edison (EDS), and Livermore (LVF). These stations experienced the highest hourly ozone concentrations observed in the Sacramento non-attainment area, the northern San Joaquin Valley, the southern San Joaquin Valley, and the San Francisco Bay Area, respectively, during July 30-August 1, 2000 (see Table 3-1). Also shown are the time series comparisons of observed and modeled NO_x, CO and reactive odd nitrogen (NO_y) concentrations at stations where measurements are available for those species; NO_y, which represents the sum of NO_x and their oxidation products, provides an important conserved measure of the total oxidized nitrogen content in the atmosphere.

The hourly concentrations of ozone simulated by CMAQ-Base and CMAQ-APT are very similar at all four locations. In general, the diurnal pattern in observed ozone concentrations during July 30-31, 2000 is reproduced by the models. However, the peak surface ozone concentration is significantly under-estimated in both the base and plume-in-grid simulations on July 31 at SGS, EDS and LVF, and on August 1 at SGS, PLR and EDS. The peak ozone prediction on August 1, 2000 is more accurate at LVF than at the other locations. The comparisons of observed NO_x and CO concentrations (where available) with predicted values shows that the peak concentrations of these species are also generally under-estimated in both the base and PiG simulations. In particular, the

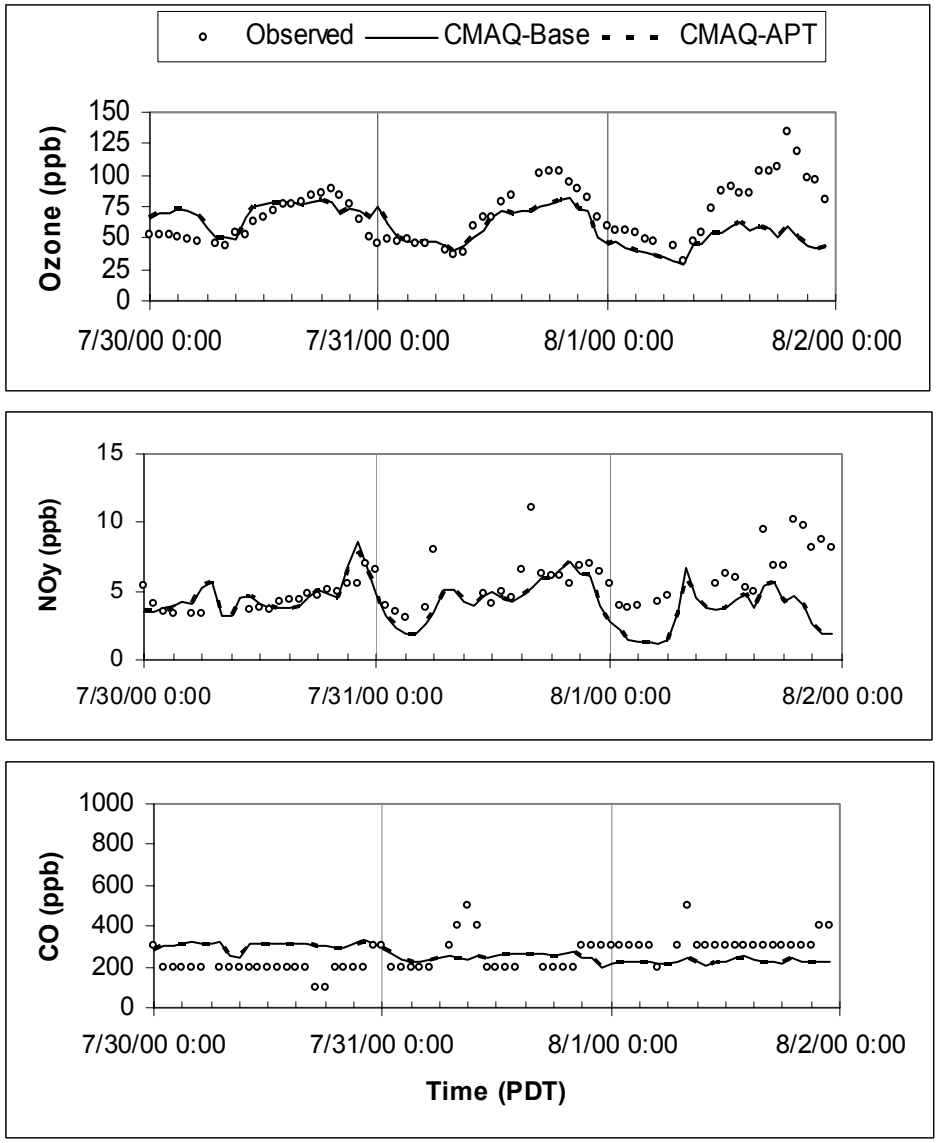

Figure 4-1. Time series of observed and modeled hourly surface concentrations of O_3, NO_y and CO at San Andreas Station (SGS) during July 30-August 1, 2000.

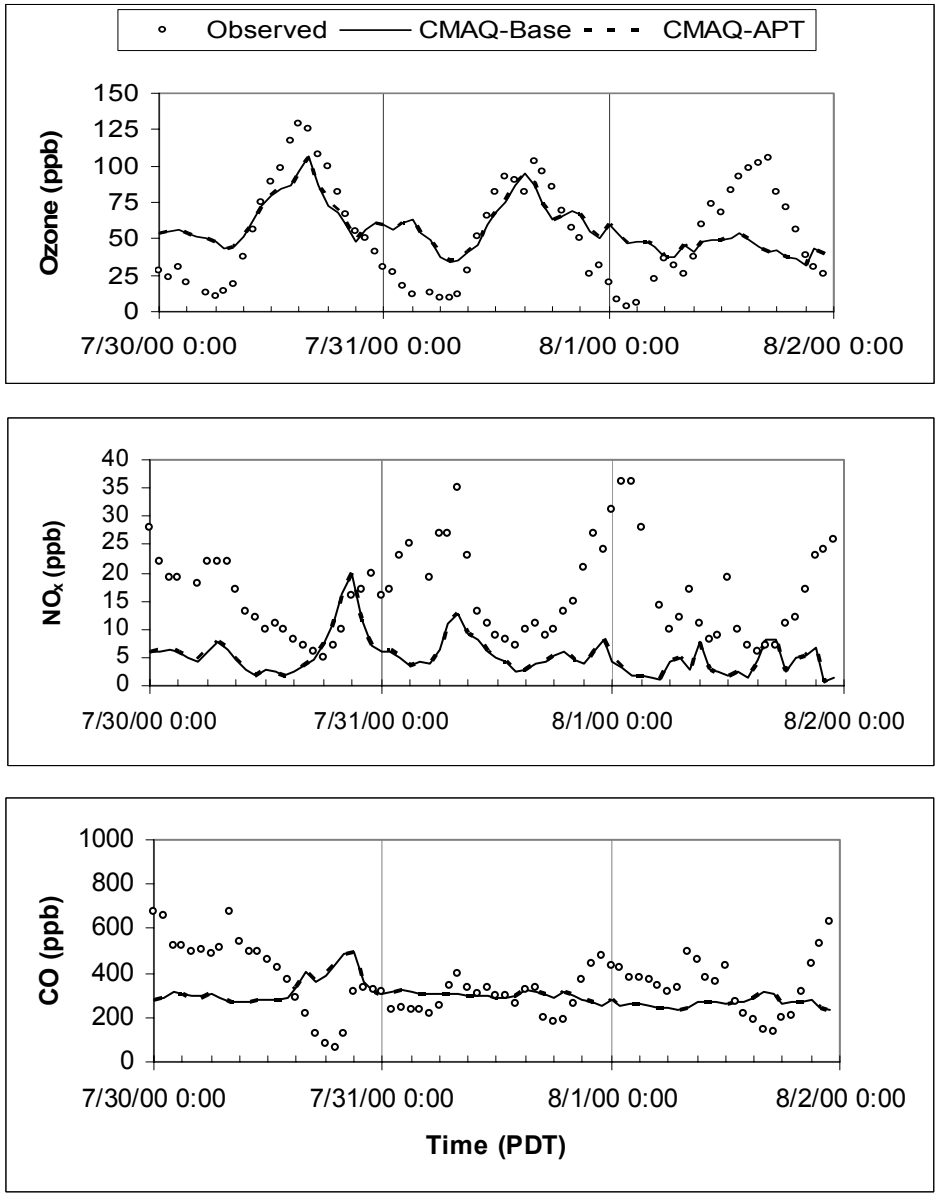

Figure 4-2. Time series of observed and modeled hourly surface concentrations of O_3, NO_x and CO at Parlier Station (PLR) during July 30-August 1, 2000.

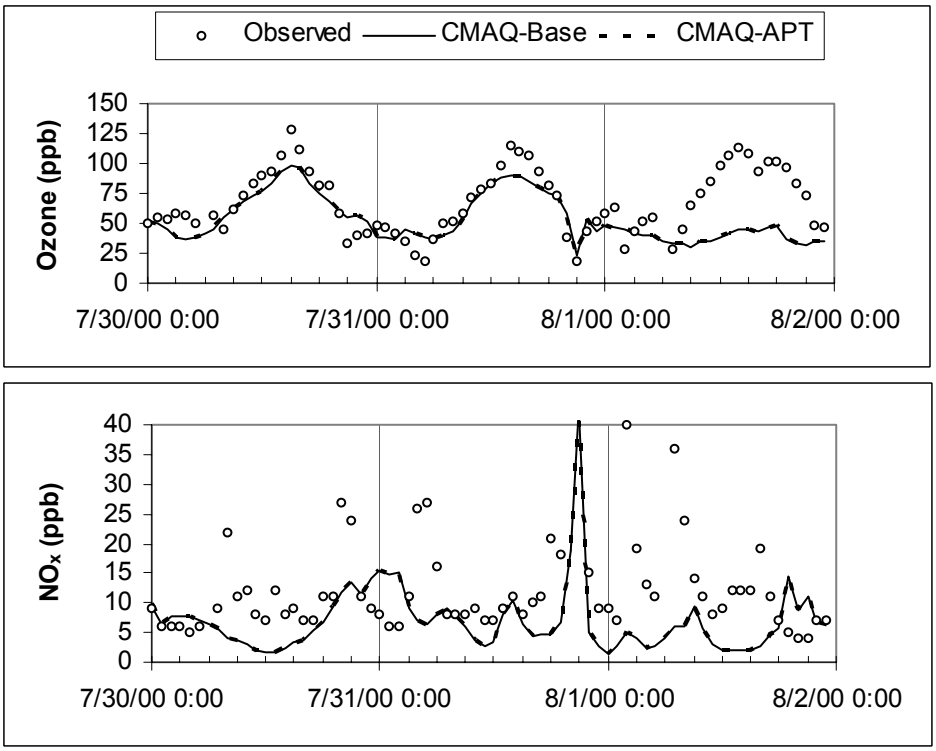

Figure 4-3. Time series of observed and modeled hourly surface concentrations of O_3 and NO_x at Edison (EDS) during July 30-August 1, 2000.

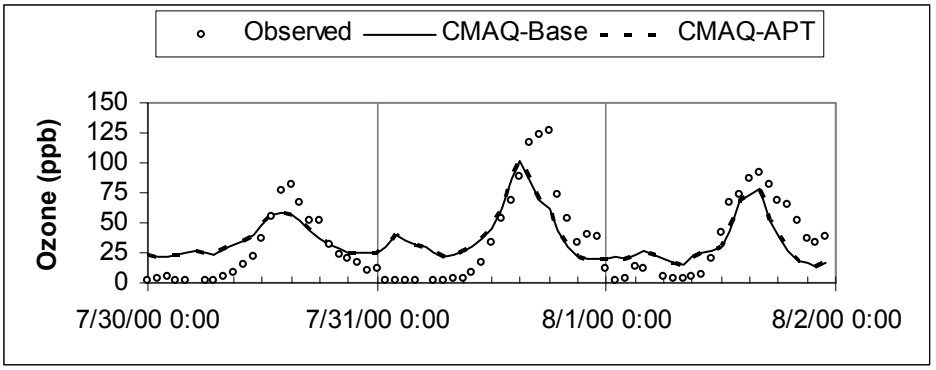

Figure 4-4. Time series of observed and modeled hourly surface concentrations of O_3 at Livermore (LVF) during July 30-August 1, 2000.

NO_x concentrations are consistently under-predicted. Note that NO_x measurements at rural locations such as Edison may be over-estimated due to interference from PAN and other oxides of nitrogen (Seinfeld and Pandis, 1998). Moreover, CO measurements may be high due to the impact of local mobile emissions which are otherwise diluted into the grid volume by the model. NO_y peaks are also generally underpredicted, but observed and simulated hourly surface NO_y concentrations at SGS are in good agreement on July 30 and July 31, 2000, as shown in Figure 4-1.

It is likely that errors in the meteorological fields used in the air quality simulations may contribute in part to the under-predictions of peak concentrations of ozone and other species. As discussed in Section 3.4, the meteorological inputs used in this study were derived from results from a simulation with MM5. The California Air Resources Board has reported that the performance of another air quality model, CAMx, was superior when using CALMET/MM5 hybrid meteorology rather than MM5 alone, since the former best utilizes the available CCOS meteorological measurements and takes advantage of the physics in MM5 (ARB, 2004). Note that this hybrid meteorology was not available to us for the study described here.

Figure 4-5 shows the time series of hourly spatial mean concentrations of observed and modeled O_3 during July 30-August 1, 2000. At any hour, the spatial mean observation is calculated from the arithmetic average of the individual concentrations at all monitoring sites within the CCOS domain. The modeled spatial mean is computed from the predictions at the same stations where measurements are reported. As seen in Figure 4-5, there is good agreement between observed and predicted spatially-averaged ozone concentrations on the first day, but model performance tends to deteriorate on the second and third days.

Figure 4-6 shows a scatter-plot comparing observed hourly ozone concentrations at all CCOS stations during July 30-August 1, 2000 with predictions from the CMAQ simulation. Figure 4-7 shows the corresponding comparison for the CMAQ-APT simulation. We see from these figures that the results from both simulations are very similar, with a coefficient of determination (R^2) of 0.31.

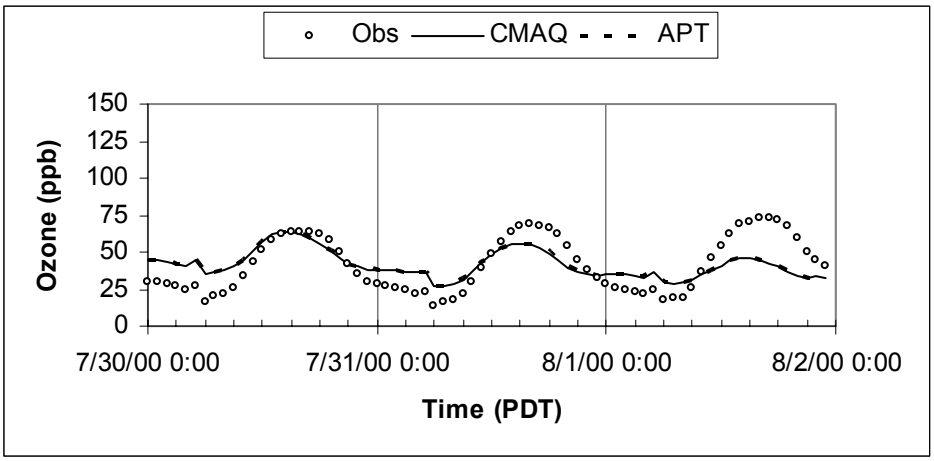

Figure 4-5 Time series of hourly spatial mean concentrations of observed and modeled O_3 during July 30-August 1, 2000.

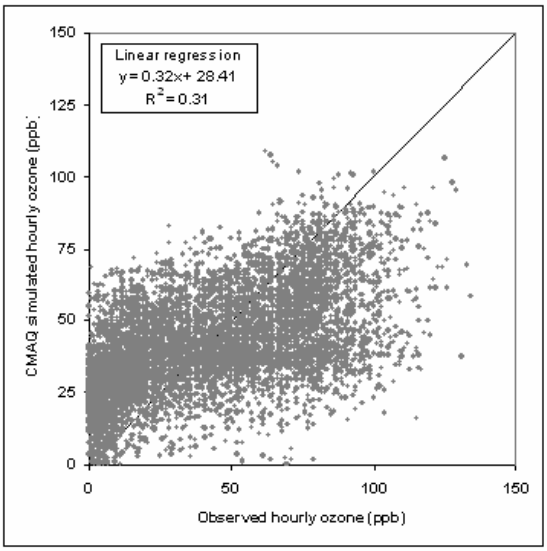

Figure 4-6. Scatterplot of hourly observed ozone vs. ozone simulated by CMAQ at all CCOS stations during July 30-August 1, 2000.

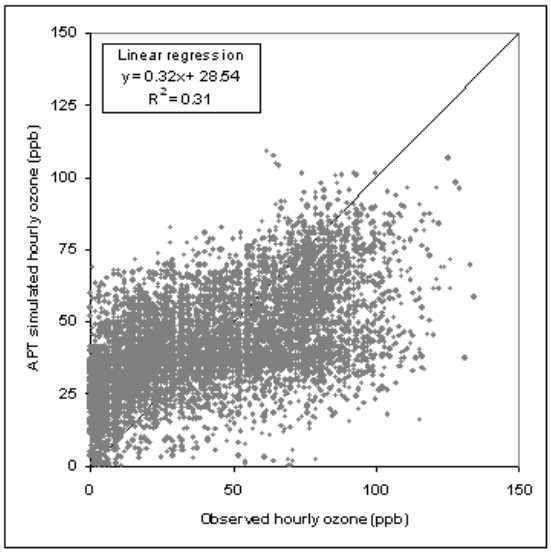

Figure 4-7. Scatterplot of hourly observed ozone vs. ozone simulated by CMAQ-APT at all CCOS stations during July 30-August 1, 2000.

A quantile-quantile (Q-Q) plot is one of the graphical measures recommended by the U.S. EPA (EPA, 1991; 1999) for evaluating the performance of ozone models. This measure compares the sorted distributions of measured and simulated ozone concentrations across the complete range of values. The measurements and predictions are not paired in time or space. Q-Q plots show whether there is any part of the distribution of observations for which the model performs poorly as indicated by significant departures from the 1:1 line at any concentration level.

Figures 4-8 and 4-9 present Q-Q plots for hourly observed ozone concentrations vs. those simulated by CMAQ and CMAQ-APT, respectively, during July 30–August 1, 2000. Again, we see that the model performance results for both simulations are very similar. The models systematically over-predict the low ozone concentrations (< 40 ppb) and under-predict the high concentrations.

In addition to errors in the meteorological fields used in the air quality simulations, there may be other reasons for the general under-prediction of peak ozone concentrations. For example, Tesche et al. (2004) have used process analysis results from CAMx simulations of the July/August 2000 CCOS episode to conclude that errors in the VOC speciation in the emissions inventory are likely responsible for inadequate hydroxyl (OH) radicals, resulting in under-estimation of ozone. These errors, if verified, would apply to the study described here as well since we used an emissions inventory similar to that used by Tesche et al. (2004).

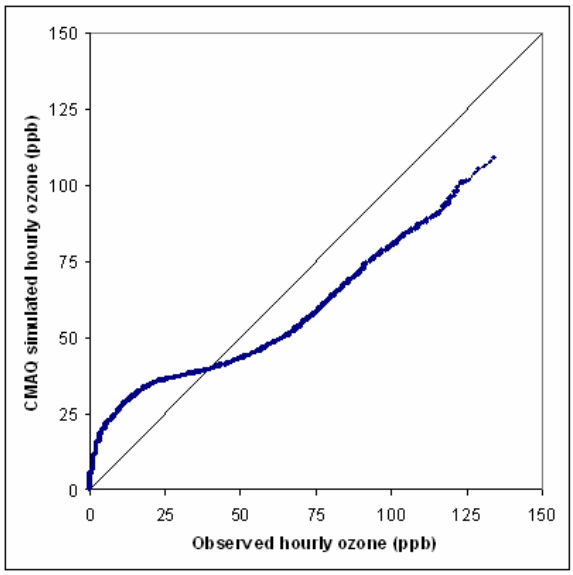

Figure 4-8. Quantile-quantile plot of hourly observed ozone vs. ozone simulated by CMAQ at all CCOS stations during July 30-August 1, 2000.

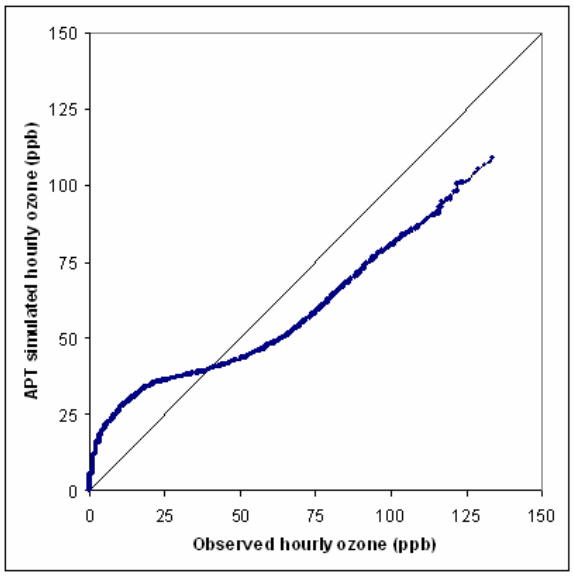

Figure 4-9. Quantile-quantile plot of hourly observed ozone vs. ozone simulated by CMAQ-APT at all CCOS stations during July 30-August 1, 2000

4.2. Statistical Performance Measures

The large and geographically diverse CCOS modeling domain was subdivided into nine sub-regions (see Figure 4-10) for model performance evaluation following the methodology adopted by ARB (2004). Statistical metrics for model performance assessments were calculated for the whole domain and for each sub-region. The sub-regions are: (1) Pacific Ocean, (2) North Coast, (3) San Francisco Bay Area, (4) Central Coast, (5) northern Sacramento Valley, (6) Sacramento/Delta, (7) Fresno area, (8) Kern County area including Bakersfield, and (9) other areas. Of these, the sub-regions of interest to the ARB (Jackson, 2004) are the San Francisco Bay Area (sub-region 3), Sacramento/Delta (sub-region 6), Fresno area (sub-region 7) and the Kern County/Bakersfield area (sub-region 8). In this section, we present statistical measures for these four sub-regions and for the entire domain.

The three most widely used multi-site metrics for ozone are the normalized bias in unpaired 1-hour daily maximum concentrations (unpaired peak accuracy), normalized bias, and normalized error, as recommended by the U.S. EPA (EPA, 1999). Table 4-1 lists these and other statistical measures for 1-hour ozone model performance using CMAQ during July 30–August 1, 2000. The normalized error, fractional error, normalized bias, fractional bias, observed peak, simulated peak, and unpaired peak accuracy of hourly surface ozone concentrations are shown for sub-regions 3, 6, 7, 8, and the entire CCOS domain in parts (a) through (e) respectively. The corresponding metrics for the CMAQ-APT simulation are presented in Table 4-2. The definitions of these statistical measures have been provided by Seigneur et al. (2000). Following ARB (2004), a cutoff value of 60 ppb was used in the calculation of ozone statistics, i.e., only observations above 60 ppb were included when computing the metrics. A total of 111 ozone monitoring stations, i.e., all those that had at least one ozone measurement exceeding the cutoff value, were used for model evaluation.

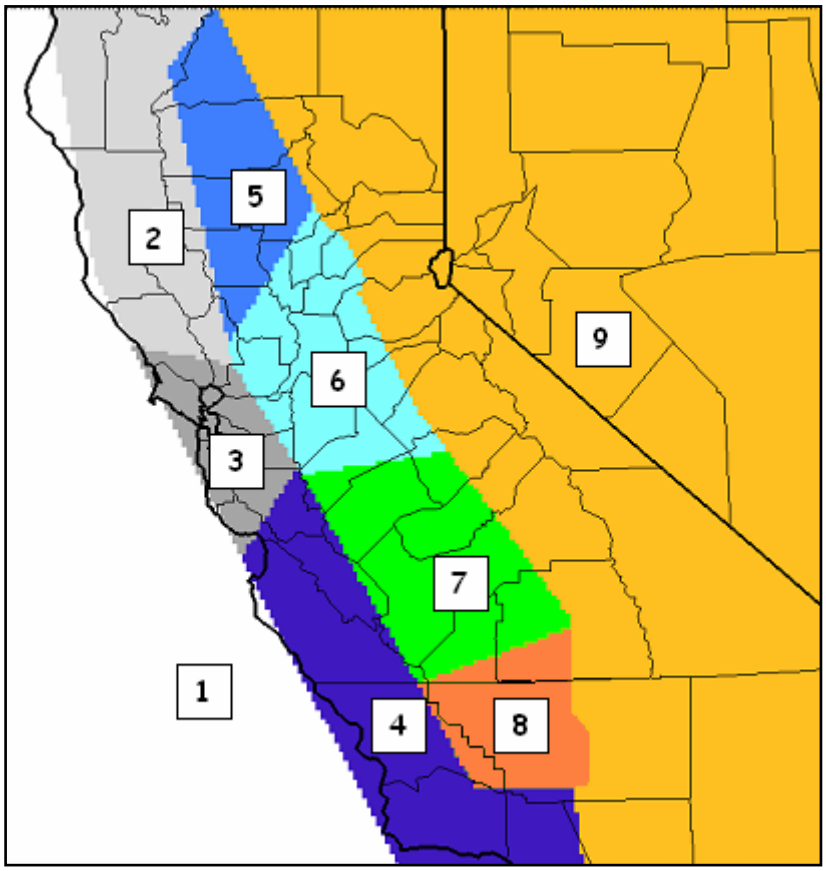

Figure 4-10. Sub-regions used in the model performance evaluation (based on ARB, 2004).

Table 4-1. 1-hour ozone model performance using CMAQ with MM5 meteorology during July 30-August 1, 2000 in: (a) sub-region 3 (SF Bay Area), (b) sub-region 6 (Sacramento/Delta area), (c) sub-region 7 (Fresno area), (d) sub-region 8 (Bakersfield area), and (e) all stations.

(a)

Date	Normalized Error (%)	Fractional Error	Normalized Bias (%)	Fractional Bias	Obs. Peak (ppb)	Sim. Peak (ppb)	Unpaired Peak Accuracy (%)
07/30/2000	27.6	0.34	-27.6	-0.34	82.0	81.1	-1.1
07/31/2000	29.8	0.36	-13.8	-0.22	126.0	115.5	-8.3
08/01/2000	43.6	0.59	-43.6	-0.59	109.0	89.0	-18.3

(b)

Date	Normalized Error (%)	Fractional Error	Normalized Bias (%)	Fractional Bias	Obs. Peak (ppb)	Sim. Peak (ppb)	Unpaired Peak Accuracy (%)
07/30/2000	15.5	0.16	-3.9	-0.06	121.0	118.5	-2.1
07/31/2000	23.8	0.29	-22.7	-0.28	110.0	114.1	3.7
08/01/2000	41.5	0.55	-41.5	-0.55	134.0	93.2	-30.4

(c)

Date	Normalized Error (%)	Fractional Error	Normalized Bias (%)	Fractional Bias	Obs. Peak (ppb)	Sim. Peak (ppb)	Unpaired Peak Accuracy (%)
07/30/2000	18.6	0.21	-15.8	-0.19	129.0	111.0	-14.0
07/31/2000	25.5	0.31	-23.0	-0.29	118.0	107.5	-8.9
08/01/2000	56.0	0.80	-56.0	-0.80	118.0	94.9	-19.6

(d)

Date	Normalized Error (%)	Fractional Error	Normalized Bias (%)	Fractional Bias	Obs. Peak (ppb)	Sim. Peak (ppb)	Unpaired Peak Accuracy (%)
07/30/2000	24.3	0.31	-24.2	-0.31	128.0	103.2	-19.4
07/31/2000	31.4	0.44	-30.7	-0.43	115.0	111.9	-2.7
08/01/2000	61.1	0.89	-61.1	-0.89	116.0	72.5	-37.5

(e)

Date	Normalized Error (%)	Fractional Error	Normalized Bias (%)	Fractional Bias	Obs. Peak (ppb)	Sim. Peak (ppb)	Unpaired Peak Accuracy (%)
07/30/2000	21.0	0.25	-16.4	-0.21	131.0	228.0	74.0
07/31/2000	30.9	0.39	-29.5	-0.38	126.0	115.5	-8.3
08/01/2000	46.7	0.63	-46.6	-0.63	134.0	97.6	-27.2

Table 4-2. 1-hour ozone model performance using CMAQ-APT with MM5 meteorology during July 30-August 1, 2000 in: (a) sub-region 3 (SF Bay Area), (b) sub-region 6 (Sacramento/Delta area), (c) sub-region 7 (Fresno area), (d) sub-region 8 (Bakersfield area), and (e) all stations.

(a)

Date	Normalized Error (%)	Fractional Error	Normalized Bias (%)	Fractional Bias	Obs. Peak (ppb)	Sim. Peak (ppb)	Unpaired Peak Accuracy (%)
07/30/2000	27.5	0.33	-27.5	-0.33	82.0	81.1	-1.1
07/31/2000	30.3	0.37	-13.1	-0.21	126.0	115.5	-8.3
08/01/2000	43.5	0.59	-43.5	-0.59	109.0	89.0	-18.3

(b)

Date	Normalized Error (%)	Fractional Error	Normalized Bias (%)	Fractional Bias	Obs. Peak (ppb)	Sim. Peak (ppb)	Unpaired Peak Accuracy (%)
07/30/2000	15.4	0.16	-3.9	-0.06	121.0	118.5	-2.1
07/31/2000	23.8	0.29	-22.3	-0.28	110.0	114.1	3.7
08/01/2000	41.2	0.55	-41.1	-0.55	134.0	93.2	-30.4

(c)

Date	Normalized Error (%)	Fractional Error	Normalized Bias (%)	Fractional Bias	Obs. Peak (ppb)	Sim. Peak (ppb)	Unpaired Peak Accuracy (%)
07/30/2000	18.4	0.21	-15.5	-0.18	129.0	111.0	-14.0
07/31/2000	25.3	0.31	-22.8	-0.28	118.0	107.5	-8.9
08/01/2000	55.9	0.79	-55.9	-0.79	118.0	94.9	-19.6

(d)

Date	Normalized Error (%)	Fractional Error	Normalized Bias (%)	Fractional Bias	Obs. Peak (ppb)	Sim. Peak (ppb)	Unpaired Peak Accuracy (%)
07/30/2000	23.9	0.30	-23.9	-0.30	128.0	103.2	-19.4
07/31/2000	31.1	0.43	-30.4	-0.43	115.0	111.9	-2.7
08/01/2000	61.1	0.89	-61.1	-0.89	116.0	72.5	-37.5

(e)

Date	Normalized Error (%)	Fractional Error	Normalized Bias (%)	Fractional Bias	Obs. Peak (ppb)	Sim. Peak (ppb)	Unpaired Peak Accuracy (%)
07/30/2000	20.8	0.25	-16.3	-0.21	131.0	228.0	74.0
07/31/2000	30.7	0.39	-29.1	-0.38	126.0	115.5	-8.3
08/01/2000	46.5	0.63	-46.5	-0.63	134.0	97.6	-27.2

As shown in Table 4-1, the best model performance for ozone concentrations is obtained in the Sacramento/Delta area (sub-region 6). The normalized errors for this sub-region are 16% and 24% on July 30 and 31, 2000, well within the EPA recommended performance goal of 35% (EPA, 1991). Unpaired peak prediction accuracy in this sub-region is -2% and 4% on these two days, again significantly better than EPA's ±20% goal. The normalized bias is -4% on July 30, 2000, which falls well within EPA's recommended value of ±15%. The performance of CMAQ on July 30, 2000 in sub-region 6 is significantly better than that exhibited by CAMx (ARB, 2004). The latter shows a normalized error of 19%, normalized bias of 13%, and unpaired peak accuracy of 31%. However, the performance of CAMx at some other locations and times is better than that of CMAQ. This is likely, in part, due to the use of the improved hybrid CALMET/MM5 meteorology in the CAMx simulation.

CMAQ does not meet EPA's one-hour ozone criteria on August 1, 2000 in any of the sub-regions. While normalized error is acceptable (less than 32%) on July 30 and 31 in all sub-regions, it is higher than 40% on August 1, 2000. The model consistently exhibits a significant negative bias ranging from -4% to -61%. The domain-wide unpaired peak accuracy on July 30, 2000 is very high (74%) due to the influence of wildfires with high NO_x emissions on simulated ozone concentrations.

Fractional error and bias are used to alleviate the problem of giving more weight to over-predictions than under-predictions, which is associated with the normalized error and bias. In this study, the fractional error and bias follow the trends exhibited by normalized error and bias since there is systematic under-prediction by the model. In an independent study of the July/August 2000 CCOS episode, Tonnesen (2003) has reported under-predictions in ozone simulated by both CMAQ and CAMx with MM5 meteorology in the southern part of the CCOS domain including the San Joaquin valley.

The ozone performance metrics for the CMAQ-APT simulation (Table 4-2) are slightly better than or comparable to those from the CMAQ simulation. The largest differences between the two simulations are seen on July 31, 2000 when the statistical measures from CMAQ-APT are about 0.5% better than those from CMAQ modeling. The peak

prediction accuracy is identical for the two models since the ozone peaks are simulated well away from the ten point sources selected for PiG treatment. The overall similarity in the model performances of CMAQ and CMAQ-APT is likely due to the fact that the NO_x emissions from the ten largest NO_x point sources (excluding wildfire emissions) selected for PiG modeling represent only a small percentage (4%) of the total NO_x emissions in the modeling domain. Furthermore, a majority of the CCOS monitoring stations are not impacted by these ten point sources. Thus, using a PiG treatment appears to have a negligible effect on predicted ozone concentrations at the CCOS monitoring locations.

Tables 4-3 and 4-4 present statistical measures for 8-hour average ozone simulated by CMAQ and CMAQ-APT, respectively. As before, a cutoff value of 60 ppb was used in the calculation of ozone statistics. As in the case of the 1-hour ozone concentrations, model performance for 8-hour ozone concentrations is best in the Sacramento/Delta sub-region. Normalized errors in the CMAQ simulation are 15%, 20% and 35% on July 30, July 31, and August 1, respectively. The unpaired peak prediction accuracy in this sub-region is -5% and -16% on July 30 and 31, respectively, better than EPA's ±20% goal. The normalized bias is negligible (-1%) on July 30, 2000. For the other sub-regions, the ranges for normalized error, normalized bias, and unpaired 8-hour peak accuracy are 16% to 60%, -60% to 8%, and -56% to -10%, respectively. Over all the monitoring stations in the domain, the best 8-hour ozone performance is on July 30 with an error, bias, and unpaired peak accuracy of 18%, -13% and -11%, respectively. The ozone performance metrics using CMAQ-APT shown in Table 4-4 are comparable to those from CMAQ. The largest difference between the two models is in sub-region 3 (SF Bay Area) on July 31, 2000. The unpaired peak accuracy is -8% for the CMAQ-APT simulation and -10% for the CMAQ simulation. However, the normalized bias is higher with CMAQ-APT than with CMAQ.

To calculate the model performance statistical metrics for NO_x, NO_y and CO, we used the following cutoff values: 1 ppb for NO_x and NO_y, and 20 ppb for CO. These cutoff values are based on typical rural background surface concentrations for these species (Seinfeld and Pandis, 1998).

Table 4-3. 8-hour ozone model performance using CMAQ with MM5 meteorology during July 30 -August 1, 2000 in: (a) sub-region 3 (SF Bay Area), (b) sub-region 6 (Sacramento/Delta area), (c) sub-region 7 (Fresno area), (d) sub-region 8 (Bakersfield area), and (e) all stations.

(a)

Date	Normalized Error (%)	Fractional Error	Normalized Bias (%)	Fractional Bias	Obs. 8hr Peak (ppb)	Sim. 8hr Peak (ppb)	Unpaired Peak Accuracy (%)
07/30/2000	20.9	0.24	-20.9	-0.24	65.6	57.2	-12.7
07/31/2000	20.1	0.2	8.3	0.06	89.5	80.7	-9.8
08/01/2000	27.7	0.34	-27.7	-0.34	90.7	60.8	-32.9

(b)

Date	Normalized Error (%)	Fractional Error	Normalized Bias (%)	Fractional Bias	Obs. 8hr Peak (ppb)	Sim. 8hr Peak (ppb)	Unpaired Peak Accuracy (%)
07/30/2000	15.3	0.16	-1.5	-0.03	93.0	97.8	5.2
07/31/2000	20.3	0.24	-19	-0.23	95.8	80.4	-16.1
08/01/2000	35.0	0.44	-35	-0.44	108.8	66.3	-39.0

(c)

Date	Normalized Error (%)	Fractional Error	Normalized Bias (%)	Fractional Bias	Obs. 8hr Peak (ppb)	Sim. 8hr Peak (ppb)	Unpaired Peak Accuracy (%)
07/30/2000	16.5	0.18	-13	-0.15	106.1	85.6	-19.3
07/31/2000	21.4	0.25	-19.1	-0.23	103.6	80.9	-21.9
08/01/2000	51.7	0.71	-51.7	-0.71	109.9	51.7	-53.0

(d)

Date	Normalized Error (%)	Fractional Error	Normalized Bias (%)	Fractional Bias	Obs. 8hr Peak (ppb)	Sim. 8hr Peak (ppb)	Unpaired Peak Accuracy (%)
07/30/2000	19.8	0.24	-19.8	-0.24	98.5	85.2	-13.5
07/31/2000	21.8	0.25	-20.4	-0.24	105.3	87.5	-16.9
08/01/2000	59.6	0.86	-59.6	-0.86	104.6	45.9	-56.2

(e)

Date	Normalized Error (%)	Fractional Error	Normalized Bias (%)	Fractional Bias	Obs. 8hr Peak (ppb)	Sim. 8hr Peak (ppb)	Unpaired Peak Accuracy (%)
07/30/2000	18.5	0.21	-13.3	-0.16	110.2	97.8	-11.3
07/31/2000	27.1	0.33	-25.3	-0.31	105.3	87.5	-16.9
08/01/2000	43.5	0.58	-43.4	-0.57	109.9	75.7	-31.1

Table 4-4 8-hour ozone model performance using CMAQ-APT with MM5 meteorology during July 30 -August 1, 2000 in: (a) sub-region 3 (SF Bay Area), (b) sub-region 6 (Sacramento/Delta area), (c) sub-region 7 (Fresno area), (d) sub-region 8 (Bakersfield area), and (e) all stations.

(a)

Date	Normalized Error (%)	Fractional Error	Normalized Bias (%)	Fractional Bias	Obs. 8hr Peak (ppb)	Sim. 8hr Peak (ppb)	Unpaired Peak Accuracy (%)
07/30/2000	20.9	0.24	-20.9	-0.24	65.6	57.3	-12.7
07/31/2000	20.8	0.2	9.3	0.07	89.5	82.2	-8.2
08/01/2000	27.6	0.33	-27.6	-0.33	90.7	61.2	-32.6

(b)

Date	Normalized Error (%)	Fractional Error	Normalized Bias (%)	Fractional Bias	Obs. 8hr Peak (ppb)	Sim. 8hr Peak (ppb)	Unpaired Peak Accuracy (%)
07/30/2000	15.3	0.16	-1.4	-0.03	93.0	97.9	5.3
07/31/2000	20.3	0.24	-18.6	-0.22	95.8	80.4	-16.1
08/01/2000	34.7	0.44	-34.6	-0.44	108.8	67.2	-38.2

(c)

Date	Normalized Error (%)	Fractional Error	Normalized Bias (%)	Fractional Bias	Obs. 8hr Peak (ppb)	Sim. 8hr Peak (ppb)	Unpaired Peak Accuracy (%)
07/30/2000	16.3	0.18	-12.6	-0.14	106.1	85.9	-19.0
07/31/2000	21.2	0.24	-18.9	-0.22	103.6	81.0	-21.9
08/01/2000	51.6	0.71	-51.6	-0.71	109.9	51.8	-52.9

(d)

Date	Normalized Error (%)	Fractional Error	Normalized Bias (%)	Fractional Bias	Obs. 8hr Peak (ppb)	Sim. 8hr Peak (ppb)	Unpaired Peak Accuracy (%)
07/30/2000	19.6	0.24	-19.5	-0.24	98.5	85.5	-13.2
07/31/2000	21.5	0.25	-20.1	-0.24	105.3	87.7	-16.8
08/01/2000	59.6	0.86	-59.6	-0.86	104.6	45.9	-56.1

(e)

Date	Normalized Error (%)	Fractional Error	Normalized Bias (%)	Fractional Bias	Obs. 8hr Peak (ppb)	Sim. 8hr Peak (ppb)	Unpaired Peak Accuracy (%)
07/30/2000	18.4	0.21	-13.2	-0.16	110.2	97.9	-11.2
07/31/2000	27.0	0.33	-25.1	-0.31	105.3	87.7	-16.8
08/01/2000	43.3	0.57	-43.3	-0.57	109.9	75.2	-31.6

Tables 4-5 and 4-6 present the performance metrics for surface NO_x concentrations for CMAQ and CMAQ-APT, respectively. Both models systematically under-predict NO_x concentrations, consistent with the time series plots shown in Section 4.1 for selected monitoring locations. Statistical measures for NO_y are shown in Tables 4-7 and 4-8 for CMAQ and CMAQ-APT, respectively. The performance of CMAQ-APT is better than or comparable to that of CMAQ. For example, in sub-region 6 on July 31, 2000, the normalized error and bias are 42.2% and 17.8%, respectively, with CMAQ; they improve slightly to 39.8% and 16.4%, respectively, with CMAQ-APT. The CO performance measures (shown in Tables 4-9 and 4-10) are identical for the two models since CO concentrations are not affected by the elevated point sources selected for PiG treatment.

In summary, both CMAQ and CMAQ-APT meet the accepted model performance goals for ozone on July 30 and 31, 2000 for peak accuracy and normalized error, but tend to show large biases. Both models tend to under-predict peak ozone concentrations, particularly on August 1, 2000. Such under-predictions have been noted in previous simulations of this episode with other air quality models (ARB, 2004) and appear to be related to errors in the meteorological fields as well as possible errors in the speciated VOC emissions inventory.

The results from CMAQ and CMAQ-APT are generally similar at most of the CCOS monitoring locations, resulting in comparable model performance. The model performance statistics are slightly better for CMAQ-APT than for CMAQ. In the previous CMAQ-APT application to the northeastern United States, where the NO_x emissions from the largest point sources were an order of magnitude higher than those in the CCOS domain, the model performance for CMAQ-APT was also comparable to and slightly better than that for CMAQ (Karamchandani et al., 2002). In the next section, we examine the impact of using a plume-in-grid approach on model results downwind of the point sources resolved by the plume model.

Table 4-5. NO_x model performance using CMAQ with MM5 meteorology during July 30-August 1, 2000 in: (a) sub-region 3 (SF Bay Area), (b) sub-region 6 (Sacramento/Delta area), (c) sub-region 7 (Fresno area), (d) sub-region 8 (Bakersfield area), and (e) all stations.

(a)

Date	Normalized Error (%)	Fractional Error	Normalized Bias (%)	Fractional Bias
07/30/2000	48.0	0.70	-46.1	-0.68
07/31/2000	66.1	0.61	17.0	-0.11
08/01/2000	95.7	0.69	55.5	0.12

(b)

Date	Normalized Error (%)	Fractional Error	Normalized Bias (%)	Fractional Bias
07/30/2000	63.4	0.53	17.7	-0.10
07/31/2000	68.1	0.69	-2.2	-0.35
08/01/2000	54.7	0.68	-26.7	-0.51

(c)

Date	Normalized Error (%)	Fractional Error	Normalized Bias (%)	Fractional Bias
07/30/2000	73.5	0.70	4.5	-0.32
07/31/2000	65.0	0.75	-18.9	-0.49
08/01/2000	66.7	0.99	-44.8	-0.85

(d)

Date	Normalized Error (%)	Fractional Error	Normalized Bias (%)	Fractional Bias
07/30/2000	96.8	0.86	21.5	-0.36
07/31/2000	118.5	0.89	46.7	-0.29
08/01/2000	98.1	1.07	0.9	-0.60

(e)

Date	Normalized Error (%)	Fractional Error	Normalized Bias (%)	Fractional Bias
07/30/2000	71.9	0.84	-15.6	-0.56
07/31/2000	76.7	0.96	-25.2	-0.71
08/01/2000	74.4	1.12	-48.3	-0.98

Table 4-6. NO_x model performance using CMAQ-APT with MM5 meteorology during July 30-August 1, 2000 in: (a) sub-region 3 (SF Bay Area), (b) sub-region 6 (Sacramento/Delta area), (c) sub-region 7 (Fresno area), (d) sub-region 8 (Bakersfield area), and (e) all stations.

(a)

Date	Normalized Error (%)	Fractional Error	Normalized Bias (%)	Fractional Bias
07/30/2000	47.9	0.70	-46.1	-0.68
07/31/2000	66.0	0.61	17.0	-0.11
08/01/2000	95.8	0.69	55.5	0.12

(b)

Date	Normalized Error (%)	Fractional Error	Normalized Bias (%)	Fractional Bias
07/30/2000	62.3	0.52	17.3	-0.09
07/31/2000	67.6	0.69	-2.5	-0.35
08/01/2000	55.0	0.68	-26.9	-0.51

(c)

Date	Normalized Error (%)	Fractional Error	Normalized Bias (%)	Fractional Bias
07/30/2000	73.4	0.70	4.5	-0.32
07/31/2000	65.0	0.75	-18.8	-0.49
08/01/2000	66.7	0.99	-44.7	-0.85

(d)

Date	Normalized Error (%)	Fractional Error	Normalized Bias (%)	Fractional Bias
07/30/2000	96.8	0.86	21.6	-0.36
07/31/2000	118.5	0.89	46.8	-0.29
08/01/2000	98.1	1.07	1.0	-0.60

(e)

Date	Normalized Error (%)	Fractional Error	Normalized Bias (%)	Fractional Bias
07/30/2000	70.9	0.84	-18.4	-0.58
07/31/2000	76.8	0.96	-26.1	-0.72
08/01/2000	74.6	1.13	-48.8	-0.98

Table 4-7. NO_y model performance using CMAQ with MM5 meteorology during July 30-August 1, 2000 in: (a) sub-region 3 (SF Bay Area), (b) sub-region 6 (Sacramento/Delta area), (c) sub-region 7 (Fresno area), (d) sub-region 8 (Bakersfield area), and (e) all stations.

(a)

Date	Normalized Error (%)	Fractional Error	Normalized Bias (%)	Fractional Bias
07/30/2000	52.8	0.78	-48.0	-0.74
07/31/2000	40.5	0.55	-24.4	-0.42
08/01/2000	61.1	0.92	-61.1	-0.92

(b)

Date	Normalized Error (%)	Fractional Error	Normalized Bias (%)	Fractional Bias
07/30/2000	47.8	0.35	32.5	0.16
07/31/2000	42.2	0.36	17.8	0.06
08/01/2000	60.1	0.59	1.7	-0.22

(c)

Date	Normalized Error (%)	Fractional Error	Normalized Bias (%)	Fractional Bias
07/30/2000	88.1	0.51	85.9	0.49
07/31/2000	77.8	0.50	71.9	0.43
08/01/2000	40.9	0.38	10.9	0.00

(d)

Date	Normalized Error (%)	Fractional Error	Normalized Bias (%)	Fractional Bias
07/30/2000	52.3	0.48	6.2	-0.12
07/31/2000	56.6	0.51	11.9	-0.13
08/01/2000	73.7	1.07	-44.5	-0.89

(e)

Date	Normalized Error (%)	Fractional Error	Normalized Bias (%)	Fractional Bias
07/30/2000	56.1	0.48	19.4	-0.02
07/31/2000	50.1	0.50	5.3	-0.15
08/01/2000	59.2	0.76	-24.7	-0.54

Table 4-8. NO_y model performance using CMAQ-APT with MM5 meteorology during July 30-August 1, 2000 in: (a) sub-region 3 (SF Bay Area), (b) sub-region 6 (Sacramento/Delta area), (c) sub-region 7 (Fresno area), (d) sub-region 8 (Bakersfield area), and (e) all stations.

(a)

Date	Normalized Error (%)	Fractional Error	Normalized Bias (%)	Fractional Bias
07/30/2000	52.8	0.78	-48	-0.74
07/31/2000	40.5	0.55	-24.3	-0.42
08/01/2000	61.1	0.92	-61.1	-0.92

(b)

Date	Normalized Error (%)	Fractional Error	Normalized Bias (%)	Fractional Bias
07/30/2000	46.9	0.35	30.6	0.16
07/31/2000	39.8	0.35	16.4	0.06
08/01/2000	59.1	0.58	1.6	-0.21

(c)

Date	Normalized Error (%)	Fractional Error	Normalized Bias (%)	Fractional Bias
07/30/2000	87.2	0.51	84.7	0.48
07/31/2000	77.8	0.5	71.6	0.43
08/01/2000	40.9	0.38	11.2	0

(d)

Date	Normalized Error (%)	Fractional Error	Normalized Bias (%)	Fractional Bias
07/30/2000	52.2	0.48	6.5	-0.12
07/31/2000	56.6	0.51	12.5	-0.12
08/01/2000	73.6	1.07	-44.4	-0.88

(e)

Date	Normalized Error (%)	Fractional Error	Normalized Bias (%)	Fractional Bias
07/30/2000	55.2	0.48	18.1	-0.03
07/31/2000	49.4	0.49	4.9	-0.15
08/01/2000	58.9	0.76	-24.9	-0.54

Table 4-9. CO model performance using CMAQ with MM5 meteorology during July 30-August 1, 2000 in: (a) sub-region 3 (SF Bay Area), (b) sub-region 6 (Sacramento/Delta area), (c) sub-region 7 (Fresno area), (d) sub-region 8 (Bakersfield area), and (e) all stations.

(a)

Date	Normalized Error (%)	Fractional Error	Normalized Bias (%)	Fractional Bias
07/30/2000	44.0	0.38	12.1	-0.03
07/31/2000	44.3	0.46	-8.3	-0.24
08/01/2000	41.1	0.49	-23.0	-0.36

(b)

Date	Normalized Error (%)	Fractional Error	Normalized Bias (%)	Fractional Bias
07/30/2000	71.0	0.44	60.2	0.31
07/31/2000	37.5	0.36	5.9	-0.05
08/01/2000	40.6	0.42	-7.0	-0.21

(c)

Date	Normalized Error (%)	Fractional Error	Normalized Bias (%)	Fractional Bias
07/30/2000	51.8	0.37	32.7	0.14
07/31/2000	36.4	0.37	-1.1	-0.12
08/01/2000	39.4	0.50	-24.8	-0.38

(d)

Date	Normalized Error (%)	Fractional Error	Normalized Bias (%)	Fractional Bias
07/30/2000	75.2	0.57	27.4	-0.07
07/31/2000	69.5	0.55	26.6	-0.02
08/01/2000	75.2	0.63	15.8	-0.19

(e)

Date	Normalized Error (%)	Fractional Error	Normalized Bias (%)	Fractional Bias
07/30/2000	56.6	0.43	29.3	0.07
07/31/2000	43.5	0.46	-5.1	-0.21
08/01/2000	44.2	0.51	-18.5	-0.35

Table 4-10. CO model performance using CMAQ-APT with MM5 meteorology during July 30-August 1, 2000 in: (a) sub-region 3 (SF Bay Area), (b) sub-region 6 (Sacramento/Delta area), (c) sub-region 7 (Fresno area), (d) sub-region 8 (Bakersfield area), and (e) all stations.

(a)

Date	Normalized Error (%)	Fractional Error	Normalized Bias (%)	Fractional Bias
07/30/2000	44.0	0.38	12.1	-0.03
07/31/2000	44.3	0.46	-8.3	-0.24
08/01/2000	41.1	0.49	-23	-0.37

(b)

Date	Normalized Error (%)	Fractional Error	Normalized Bias (%)	Fractional Bias
07/30/2000	71.0	0.44	60.2	0.31
07/31/2000	37.5	0.36	5.8	-0.05
08/01/2000	40.6	0.42	-7.1	-0.21

(c)

Date	Normalized Error (%)	Fractional Error	Normalized Bias (%)	Fractional Bias
07/30/2000	51.8	0.37	32.6	0.13
07/31/2000	36.4	0.37	-1.1	-0.12
08/01/2000	39.4	0.50	-24.8	-0.38

(d)

Date	Normalized Error (%)	Fractional Error	Normalized Bias (%)	Fractional Bias
07/30/2000	75.2	0.57	27.4	-0.07
07/31/2000	69.5	0.55	26.6	-0.02
08/01/2000	75.2	0.63	15.8	-0.19

(e)

Date	Normalized Error (%)	Fractional Error	Normalized Bias (%)	Fractional Bias
07/30/2000	56.6	0.43	29.2	0.07
07/31/2000	43.6	0.46	-5.2	-0.21
08/01/2000	44.3	0.51	-18.6	-0.35

5. IMPACTS OF PLUME-IN-GRID MODELING WITH CMAQ-APT

In this section, we present the impacts of using a plume-in-grid treatment for the 10 largest NO_x-emitting plants in the CCOS domain on predicted O_3 and HNO_3 concentrations. To guide us in selecting the periods for showing these impacts, we used the CMAQ "background" simulation (i.e., a simulation without the emissions from these 10 plants) described in Section 3.7. As explained in Section 3.7, the differences in predicted concentrations from the background simulation with those from the APT and base simulations show the effects of emissions from these point sources with and without PiG treatment, respectively.

Before presenting the results, we briefly review the chemistry governing the formation of ozone and other secondary species, such as nitric acid, downwind of large NO_x point sources such as power plants and cement plants. This review provides the background necessary to interpret the results of using a PiG treatment to model such point sources.

5.1. Plume Chemistry

5.1.1. Background

Both experimental studies (e.g., Richards et al., 1981; Gillani et al., 1998) and theoretical studies (e.g., Karamchandani et al., 1998) have shown that the rates of ozone and acid formation in a plume rich in NO_x differ significantly from those in the background atmosphere. The reason for this difference between plume chemistry and background chemistry is that the high nitric oxide (NO) concentrations in the plume lead to a depletion of oxidant levels until sufficient plume dilution has taken place.

In the vicinity of power plants and other elevated NO_x sources, there is a temporary decrease in ozone levels, even during daytime conditions, due to the "titration" or "scavenging" of ozone by the high levels of NO in the near field of the plume. In this stage (defined as Stage 1 in Karamchandani et al., 1998), the photostationary state applies for $NO/NO_2/O_3$ and radical concentrations within the plume are negligible.

Farther downwind, as the plume starts to mix into the background environment and becomes diluted, radical concentrations within the plume start to increase and there is some formation of secondary acids. However at this stage of plume chemistry (Stage 2 in Karamchandani et al., 1998), NO_x concentrations in the plume are still high relative to plume VOC levels, and the formation of ozone is negligible. Even farther downwind, the plume has become sufficiently dispersed that its chemistry is qualitatively similar to that of the ambient background. In this stage (Stage 3 in Karamchandani et al., 1998), the rate of formation of ozone and secondary acids is determined by the VOC/NO_x ratios in the background environment. If the background environment is NO_x limited, formation of ozone and secondary acids may then occur faster in the plume than in the background due to the plume NO_x.

The actual durations and extents of each of these stages in the evolution of plume chemistry depend on a number of factors such as season, time of day, prevailing meteorological conditions, and VOC and ozone concentrations in the background environment (Karamchandani et al., 1998; Karamchandani and Seigneur, 1999). In a VOC-limited environment, the release of fresh NO_x emissions will result in a scavenging of ozone that may continue for large downwind distances (i.e., longer Stages 1 and 2, resulting in a delay in the onset of Stage 3). Conversely, in a NO_x-limited environment, the fresh NO_x emissions may lead to an initial scavenging of ozone and radicals, but ozone production will begin rapidly as the emissions are transported downwind.

5.1.2. Expected PiG impacts

In the absence of a PiG treatment, the NO_x emissions from an elevated point source will result in an immediate titration of surface ozone, due to the artificial dilution of stack emissions when the gridded approach is used. Furthermore, this artificial dilution will also result in Stages 2 and 3 (see Section 5.1.1 for an explanation of these stages) occurring earlier in the grid model than in a plume model. Thus, we expect to see more rapid production of nitric acid and ozone following the initial scavenging of ozone and radicals when a gridded approach is used instead of a PiG approach for elevated point sources of NO_x.

With PiG treatment, we expect the scavenging of ozone to occur at plume height initially, followed by surface scavenging at some distance downwind as the elevated plume is transported to the surface. Because the plume model represents the plume more accurately than the grid model, we expect the actual production of nitric acid and ozone (in Stages 2 and 3) to occur later in the PiG approach than in the gridded approach.

Other possible sources of differences between the gridded and PiG approaches include:

- The "numerical diffusion" introduced by the scheme used to solve advective transport in the grid model. One effect of this artificial diffusion is the unrealistic transport of emissions upwind of the source. While most contemporary numerical solvers, including the solver used in CMAQ, attempt to reduce this error, it cannot be eliminated entirely. The plume model does not suffer from this "upwinding" effect.

- In the gridded approach, the emissions may be released over several model layers, as compared to the PiG approach, where the emissions are released at the effective stack height. This may result in the plume being transported in different directions in the gridded approach vs. the PiG approach in the presence of wind shear.

5.2. Impacts on Ozone Concentrations

Figure 5-1 presents the differences between surface O_3 concentrations from the base (CMAQ Base) and background (CMAQ Background) simulations at 3 p.m. PDT on July 30, 2000 in (a) the entire domain and (b) a small sub-domain covering the extended San Francisco Bay Area. The time selected corresponds to the hour of highest differences in ozone concentrations on this day, i.e., maximum base case simulated impact due to the emission sources of interest in the modeling domain. Positive values in the plots (represented by yellow, orange, and red colors) indicate regions with ozone production (in the CMAQ Base simulation) due to the NO_x emissions from the ten point sources. Negative values (denoted by different shades of green and blue) represent titration or scavenging of ozone due to the NO_x emissions.

(a)

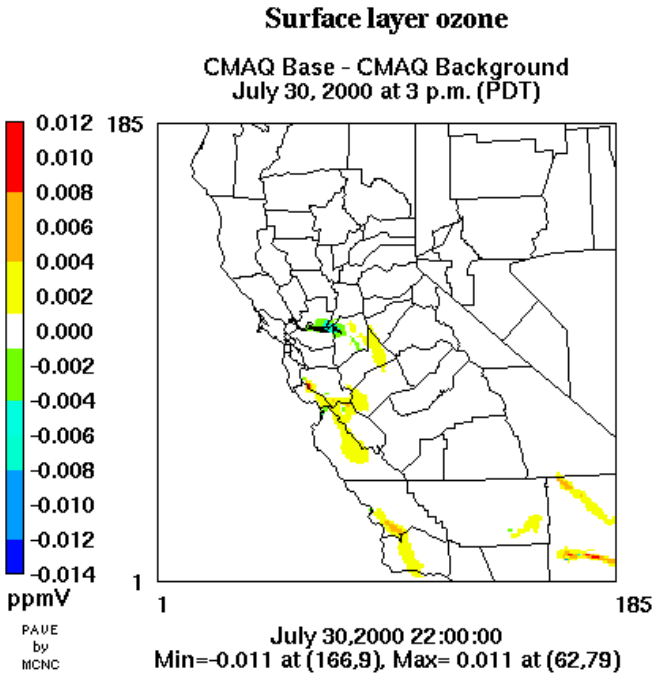

(b)

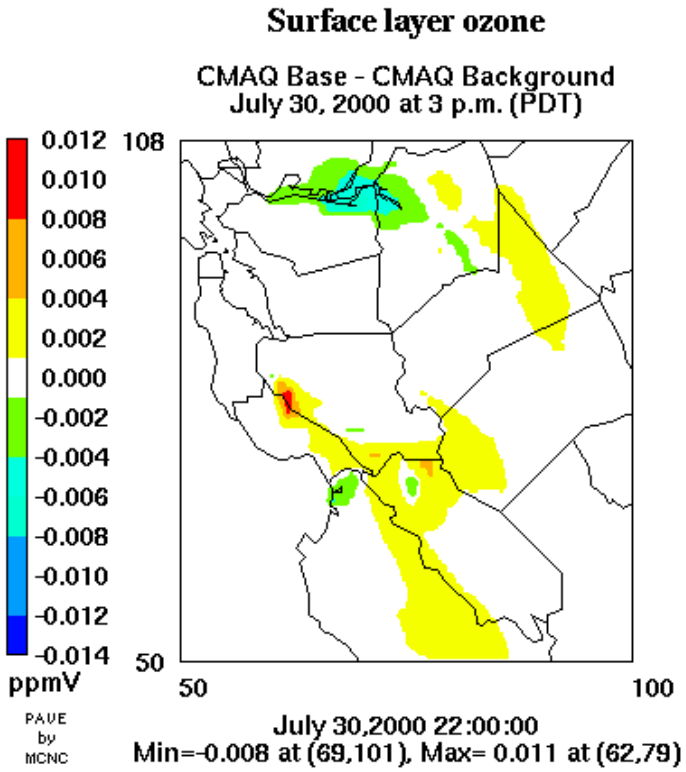

Figure 5-1. Differences (Base–Background) in surface O_3 concentrations at 3 p.m. PDT on July 30, 2000 in (a) the entire domain and (b) the extended Bay Area.

The direction of transport of the emissions and ozone production due to each of the plants can be inferred from Figure 5-1. Wind flow is generally westerly to northwesterly at the locations of the Pittsburg and Contra Costa Power Plants, Hanson Permanente Cement Plant, IMC Chemicals and the unknown plant in San Luis Obispo County. Winds are westerly or southwesterly at the locations of the other plants selected for explicit PiG treatment. This general behavior is consistent with the CCOS meteorology characterized by Lehrman et al. (2004).

The effect of the Pittsburg Power Plant and Contra Costa Power Plant (CCPP) emissions on ozone concentrations is evident in Contra Costa and San Joaquin Counties. In the grid cell containing the CCPP source, the surface ozone concentration is 59 ppb, 7 ppb lower than the local background concentration of 66 ppb. This indicates that, without PiG treatment, the NO emissions from these power plants are scavenging about 11% of the ozone at the surface in the CCCP source cell and immediately downwind of the source cell.

Figure 5-2 shows the differences between surface O_3 concentrations from the APT and background simulations at 3 p.m. PDT on July 30, 2000. As in the base simulation, the combined plume from the Pittsburg and Contra Costa Power Plants travels initially to the east and then to the southeast. We see that less ozone (6% of the background O_3) is scavenged near the source in the APT simulation than in the base simulation. Farther downwind, in southeastern San Joaquin County (about 60 to 80 km downwind of the power plants), the plume material reaches the surface, resulting in more titration of ozone in the APT simulation and up to 4 ppb lower ozone concentrations than the base case. These results are consistent with our expectations, discussed in Section 5.1.2.

(a)

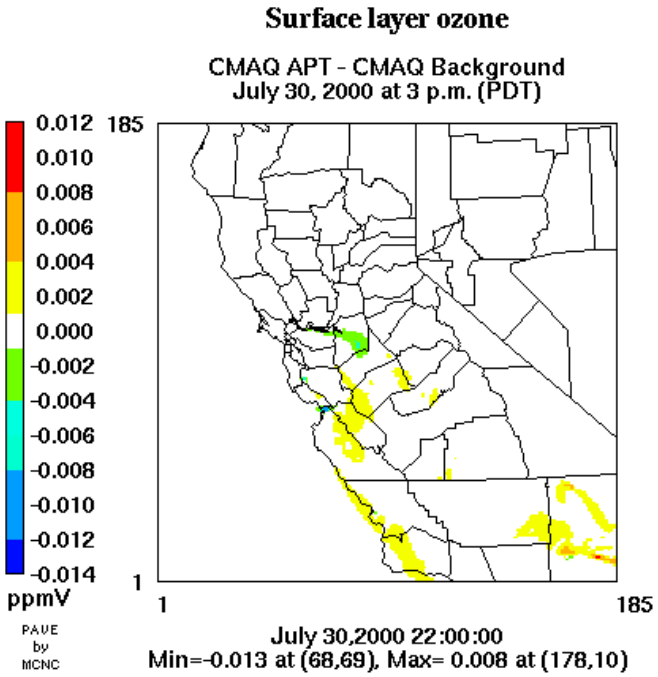

(b)

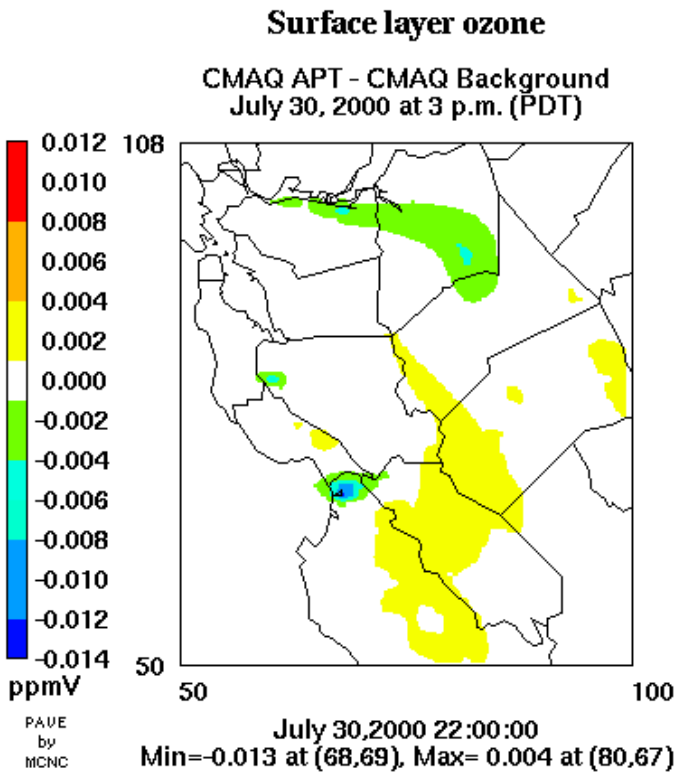

Figure 5-2. Differences (APT-Background) in surface O_3 concentrations at 3 p.m. PDT on July 30, 2000 in (a) the entire domain and (b) the extended Bay Area.

Although the general plume transport directions for the combined Pittsburg-Contra Costa plume are similar in the base case and APT simulations, there are some minor differences. In the base simulation (Figure 5-1b), some of the NO_x emissions from the Pittsburg and Contra Costa power plants are also dispersed to the north and northeast of these sources, whereas in the APT simulation all the NO_x is transported to the east and southeast (Figure 5-2b). Because the NO_x emissions initially scavenge the background ozone, as discussed in Section 5.1.1, the surface ozone concentrations simulated in the base simulation are lower than the background ozone values, and, consequently, lower than those from the APT simulation in the immediate vicinity and to the north and northeast of the sources. This is evident from Figure 5-3, which shows the differences between surface O_3 concentrations from the APT and base simulations at 3 p.m. PDT on July 30, 2000.

As discussed in Section 5.1.1, the chemistry of the background environment has a large influence on the production of ozone downwind of large NO_x sources. In particular, the relative abundance of VOC vs NO_x in the background determines whether the NO_x emissions from these sources result in ozone production, ozone destruction, or negligible changes in ozone. VOC/NO_x ratios are most often used in defining and understanding emission control strategies for ozone, but they are also useful in the context of PiG modeling and understanding the results presented here.

Blanchard and co-workers (2000; 2001) used ambient air quality data from 1991-98 to determine whether O_3 formation at specific times and locations in central California was limited by the availability of VOC or NO_x. Calculations with the Smog Production (SP) algorithm suggest that ozone formation within the San Francisco Bay Area is primarily VOC-limited. On high-ozone days, the transition between VOC and NO_x limitation typically occurred in the southern Sacramento Valley (northeast of San Francisco Bay) and the northern San Joaquin Valley. However, within inland cities such as Sacramento, Stockton, and Modesto, fresh emissions provide additional NO_x, so that locally ozone formation again becomes VOC (or radical) limited. Similarly, Fresno and Bakersfield, in the central and southern San Joaquin Valley, respectively, are locally VOC-limited, but are surrounded by larger, rural areas where ozone formation is NO_x-limited.

(a)

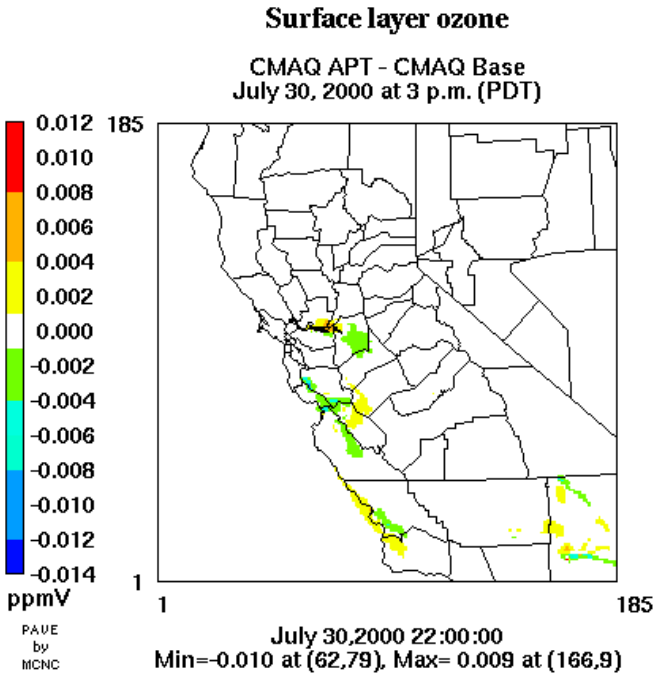

(b)

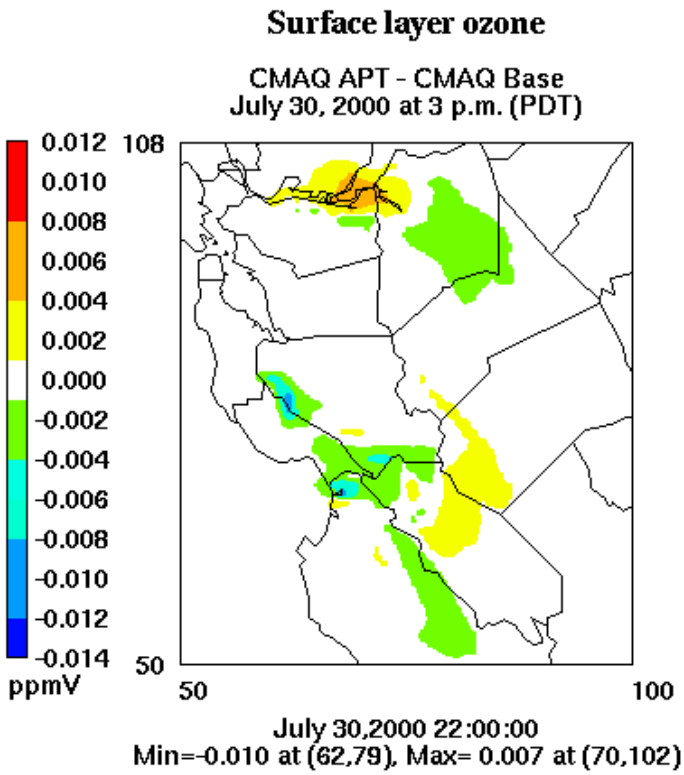

Figure 5-3. Differences (APT-Base) in surface O_3 concentrations at 3 p.m. PDT on July 30, 2000 in (a) the entire domain and (b) the extended Bay Area.

Figure 5-4 presents a compilation of mapper plots created by ARB (2004) showing the "extent of reaction" parameter from the SP algorithm at selected CCOS monitoring sites on July 30, 2000. Note that monitoring sites are not available for all counties in the domain and portions of some counties appear in multiple plots. White pies represent specific locations and times where/when the extent of reaction parameter is less than 0.5. Black pies represent areas where the extent exceeds 0.96. Blanchard and Fairley (2000) have proposed that areas where the "extent of reaction" parameter in a majority of hours is less than 0.6 are VOC-limited and those with an extent greater than 0.9 are NO_x-limited.

In general, rural areas in central California that are not near major highways or other NO_x emission sources are likely to be NO_x-limited, while urban areas, particularly those in the San Francisco Bay Area, are likely to be VOC-limited. Coastal locations in southern California are also VOC-limited. Figure 5-5 presents a map of the extended Bay Area (U.S. Census Bureau) showing major urban areas and highways. The locations of the five plants in this area that were selected for explicit PiG treatment are also shown for reference.

As discussed previously, if the background environment is VOC-limited, the effect of PiG treatment is primarily to limit titration of O_3 by NO, and this is consistent with the results presented earlier in Figures 5-1 and 5-2, where we saw that less surface ozone was titrated in the APT simulation than in the base simulation immediately downwind of the Pittsburg and the Contra Costa Power Plants. At a distance of about 60 to 80 km downwind (in eastern and southeastern San Joaquin County), we see some production of ozone in the base case simulation (Figure 5-1), while in the APT simulation, ozone titration continues, as shown in Figure 5-2. Even farther downwind (about 120 km), where the atmosphere is frequently NO_x-limited (see southeastern edge of Stanislaus County in Figure 5-2b), the APT simulation transports more NO_x to those areas than the base simulation, leading to slightly more (up to 1 ppb) ozone production in the APT simulation than in the base simulation.

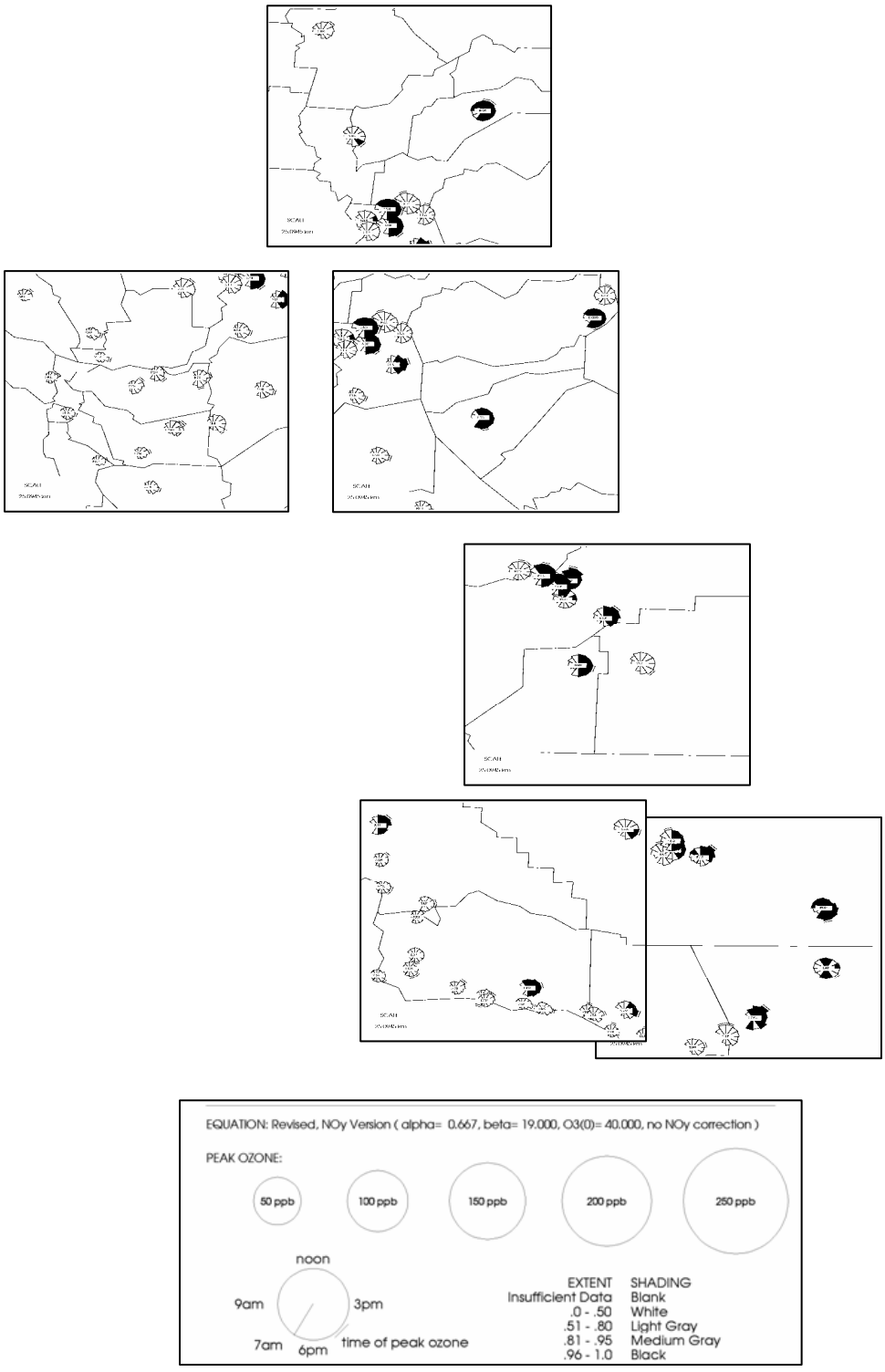

Figure 5-4. Mapper plots showing extent of reaction at selected monitoring sites in the CCOS modeling domain on July 30, 2000 (source: ARB, 2004).

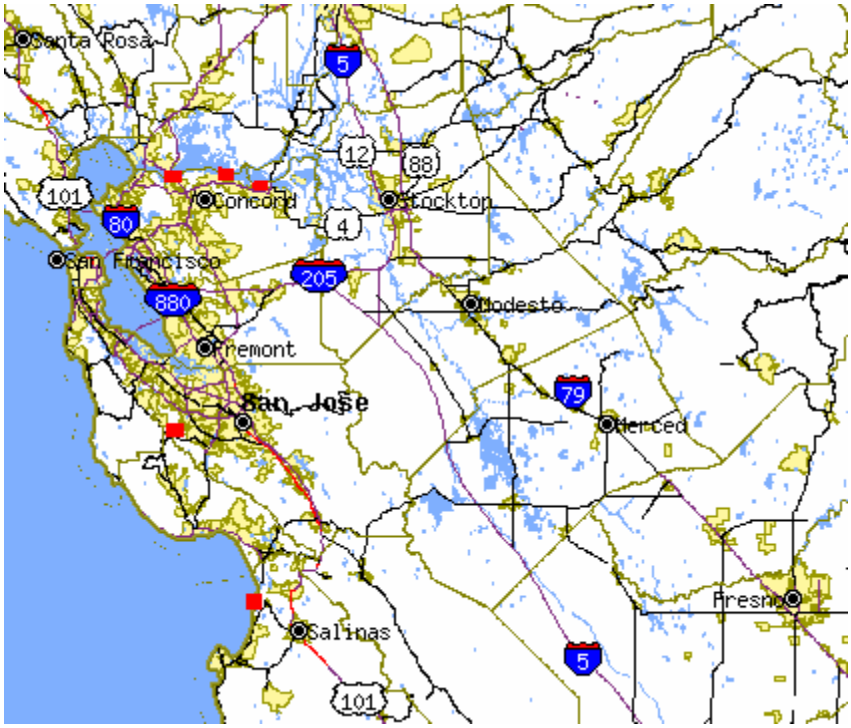

Figure 5-5. Map of the extended San Francisco Bay Area (U.S. Census Bureau, 2004). Locations of the five plants in this area selected for explicit plume-in-grid treatment are also shown by red squares.

In the base CMAQ simulation, the maximum production of ozone due to the PiG sources in the CCOS modeling domain is simulated downwind of the Hanson Permanente Cement Plant near the corner of San Mateo, Santa Cruz and Santa Clara Counties. At 3 p.m. PDT on July 30, the ozone concentration simulated by CMAQ is 11 ppb higher than the background level of 53 ppb at about 12 km downwind of the Hanson cement plant (Figure 5-1b). However, at this location, APT predicts surface ozone concentrations that are comparable to the background (Figure 5-2b). The maximum production of ozone due to the PiG sources in the CMAQ-APT simulation is 10 ppb at 4 p.m. PDT on July 30 (over a background ozone concentration of 53 ppb) near the Riverside and California Cement Plants in the southeastern part of the CCOS domain (Figure 5-2a).

The results for the Moss Landing Power Plant at 3 p.m. PDT on July 30, 2000 are qualitatively similar to those for the Pittsburg and Contra Costa power plants, although the effect of PiG treatment is less pronounced. In the base simulation (Figure 5-1b), titration of background surface ozone occurs till about 20 km downwind of the plant (to the east-north-east), followed by production of ozone of up to about 6 ppb in Monterey, San Benito and Merced Counties (compared to background values of 75 to 85 ppb). In the APT simulation, the titration occurs to a distance of about 40 km, and up to 4 ppb of ozone is produced subsequently in Monterey, San Benito and Merced Counties (Figure 5-2b).

Ozone concentration differences between base and background, between APT and background, and between APT and base at 3 p.m. PDT on July 31 are shown in Figures 5-6, 5-7, and 5-8, respectively. Similar plots at 4 p.m. PDT on August 1 are presented in Figures 5-9 through 5-11. These two times, 3 p.m. PDT on July 31 and 4 p.m. PDT on August 1, represent the hours of highest differences in ozone concentrations between the base and background CMAQ simulations on these two days (i.e., maximum base case simulated impacts due to the selected sources). Figures 5-12 and 5-13 present a compilation of mapper plots (ARB, 2004) showing the "extent of reaction" parameter from the SP algorithm at CCOS monitoring sites on July 31 and August 1, 2000, respectively.

(a)

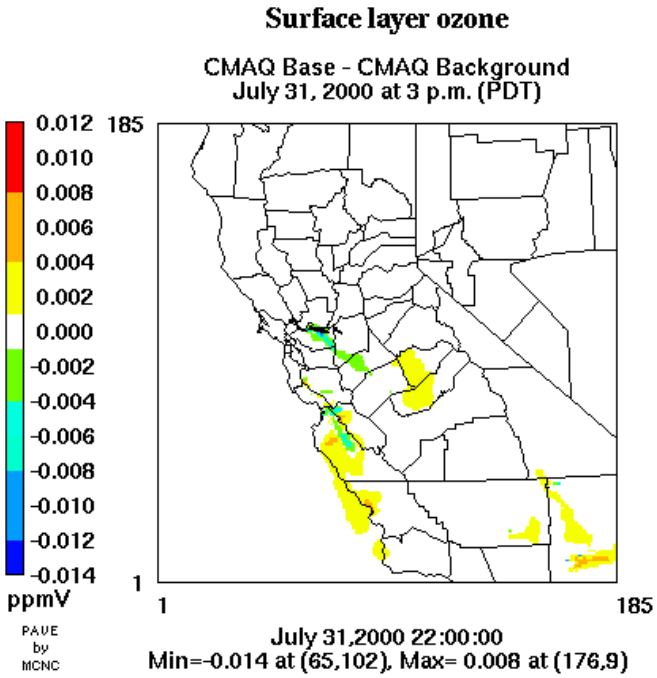

(b)

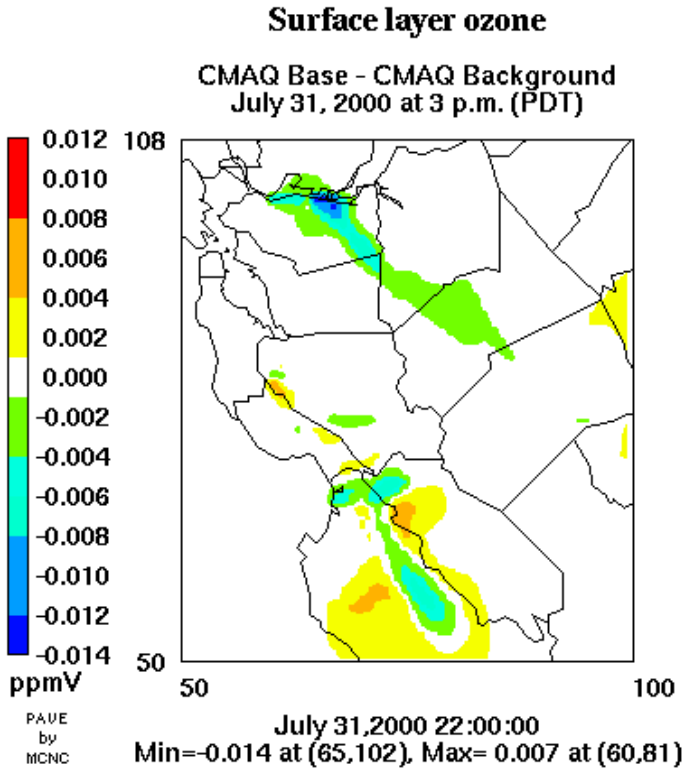

Figure 5-6. Differences (Base–Background) in surface O_3 concentrations at 3 p.m. PDT on July 31, 2000 in (a) the entire domain and (b) the extended Bay Area.

(a)

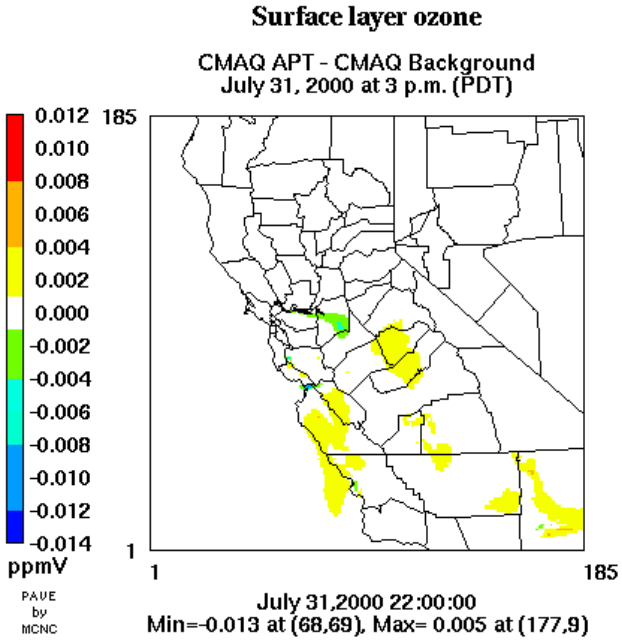

(b)

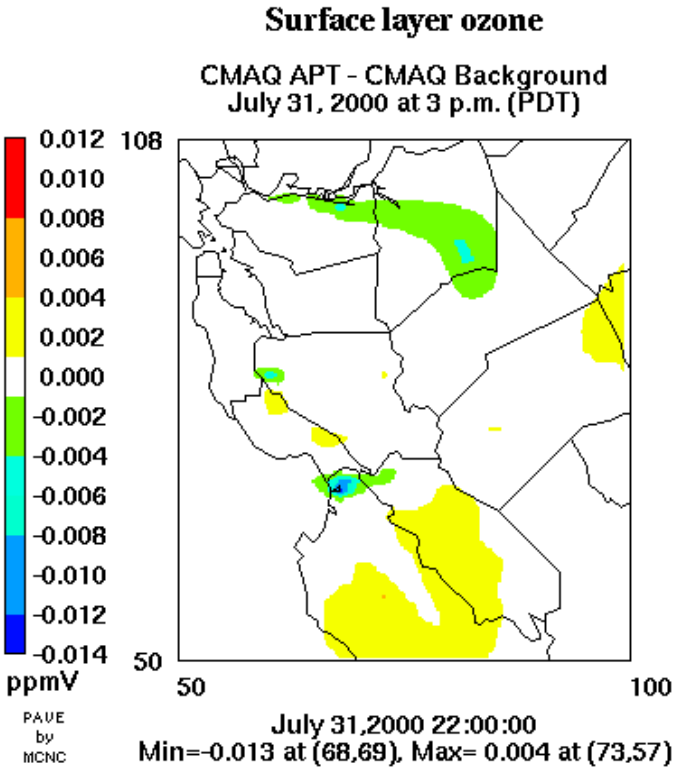

Figure 5-7. Differences (APT–Background) in surface O_3 concentrations at 3 p.m. PDT on July 31, 2000 in (a) the entire domain and (b) the extended Bay Area.

(a)

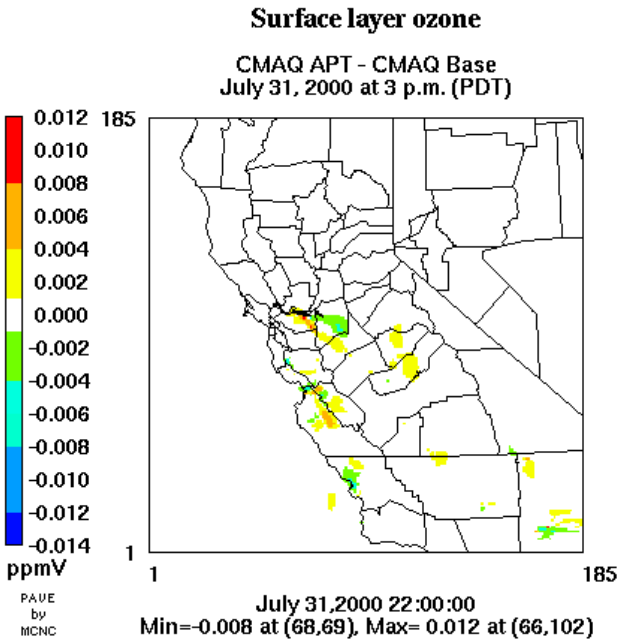

(b)

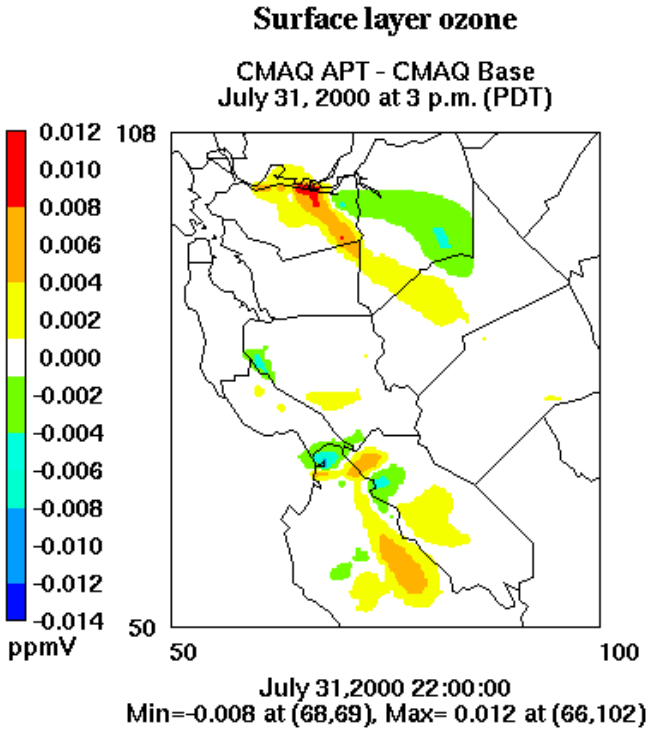

Figure 5-8. Differences (APT–Base) in surface O_3 concentrations at 3 p.m. PDT on July 31, 2000 in (a) the entire domain and (b) the extended Bay Area.

(a)

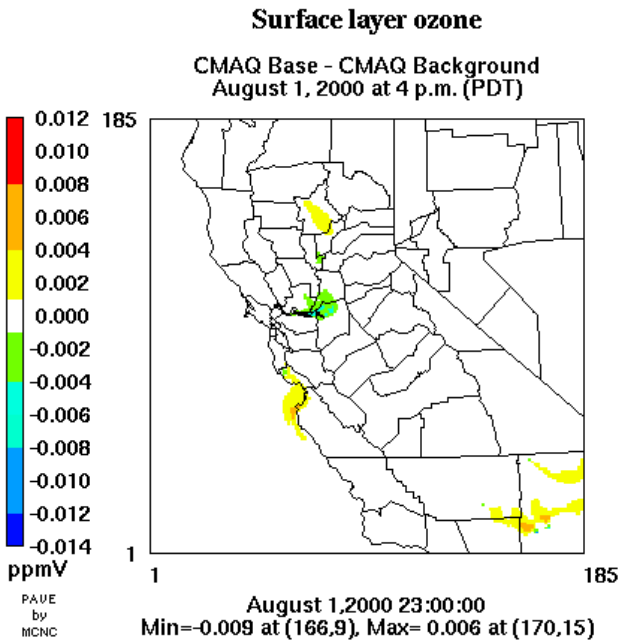

(b)

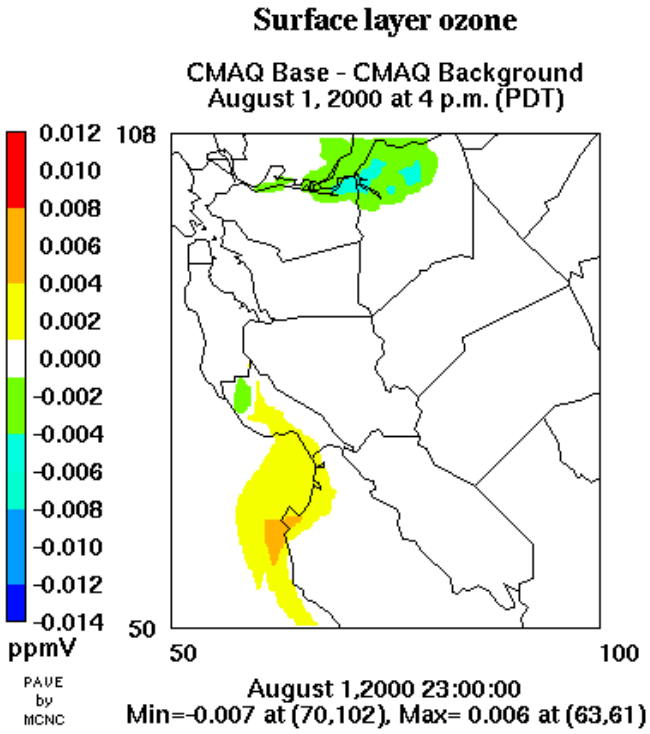

Figure 5-9. Differences (Base–Background) in surface O_3 concentrations at 4 p.m. PDT on August 1, 2000 in (a) the entire domain and (b) the extended Bay Area.

(a)

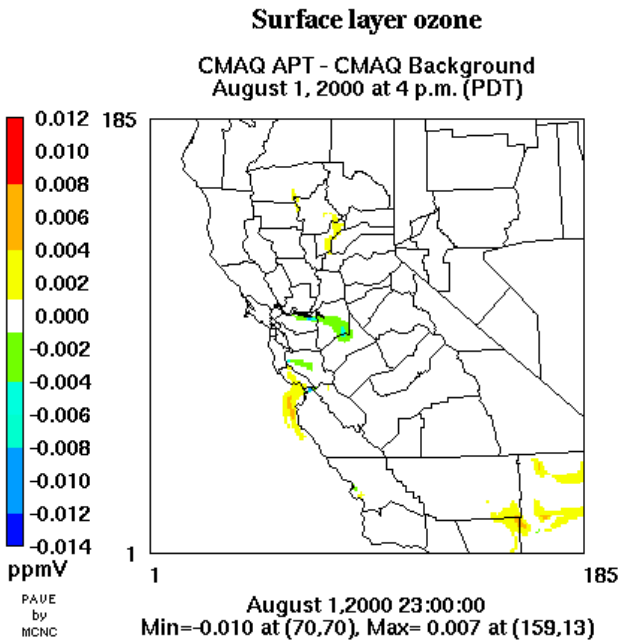

(b)

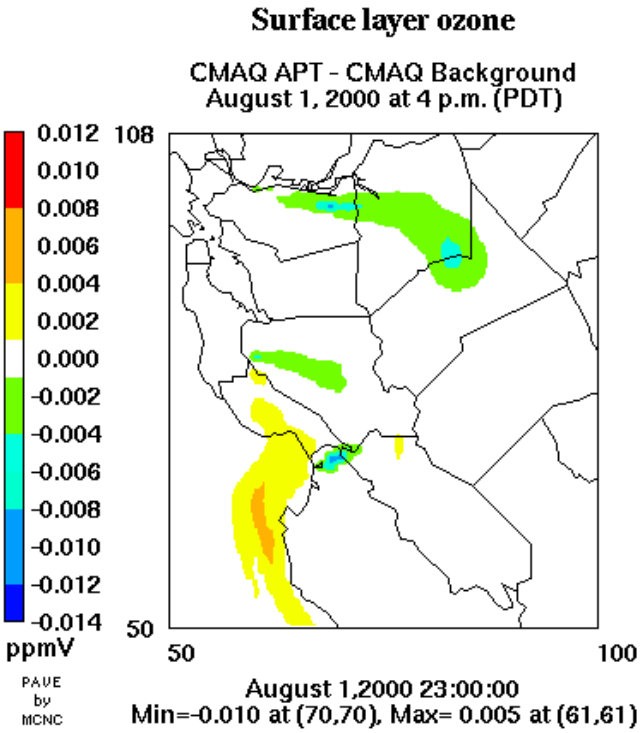

Figure 5-10. Differences (APT–Background) in surface O_3 concentrations at 4 p.m. PDT on August 1, 2000 in (a) the entire domain and (b) the extended Bay Area.

(a)

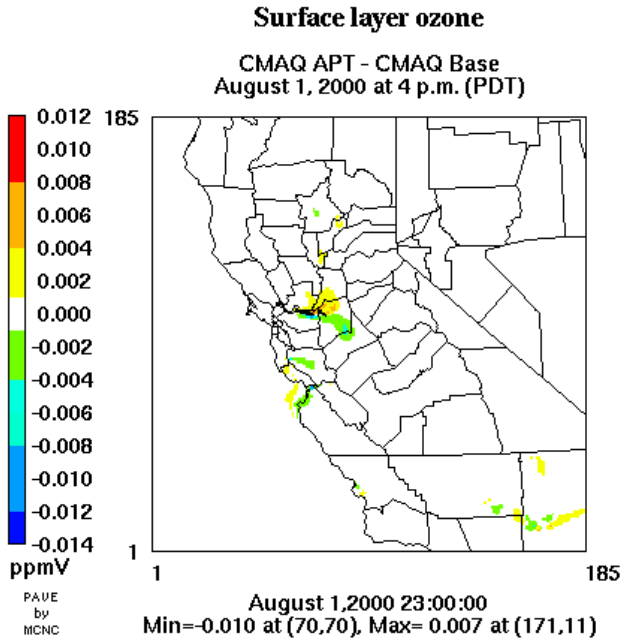

(b)

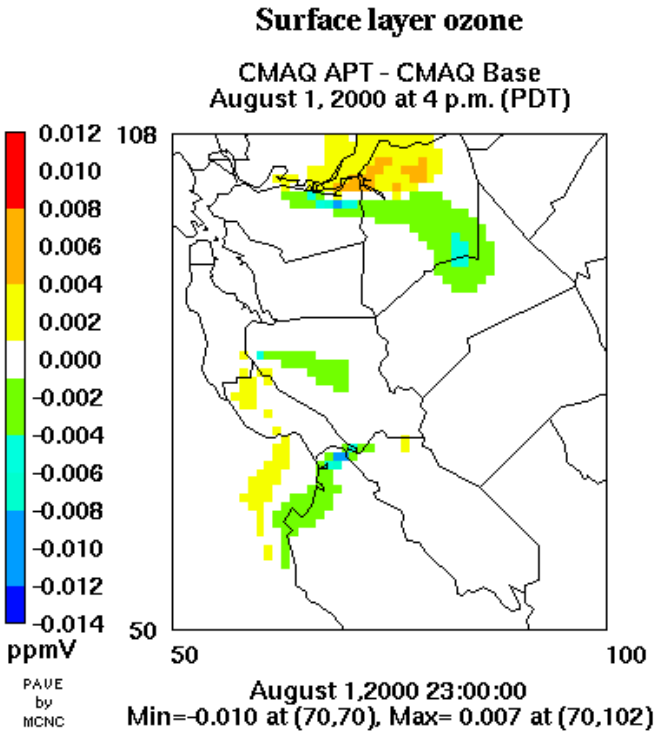

Figure 5-11. Differences (APT–Base) in surface O_3 concentrations at 4 p.m. PDT on August 1, 2000 in (a) the entire domain and (b) the extended Bay Area.

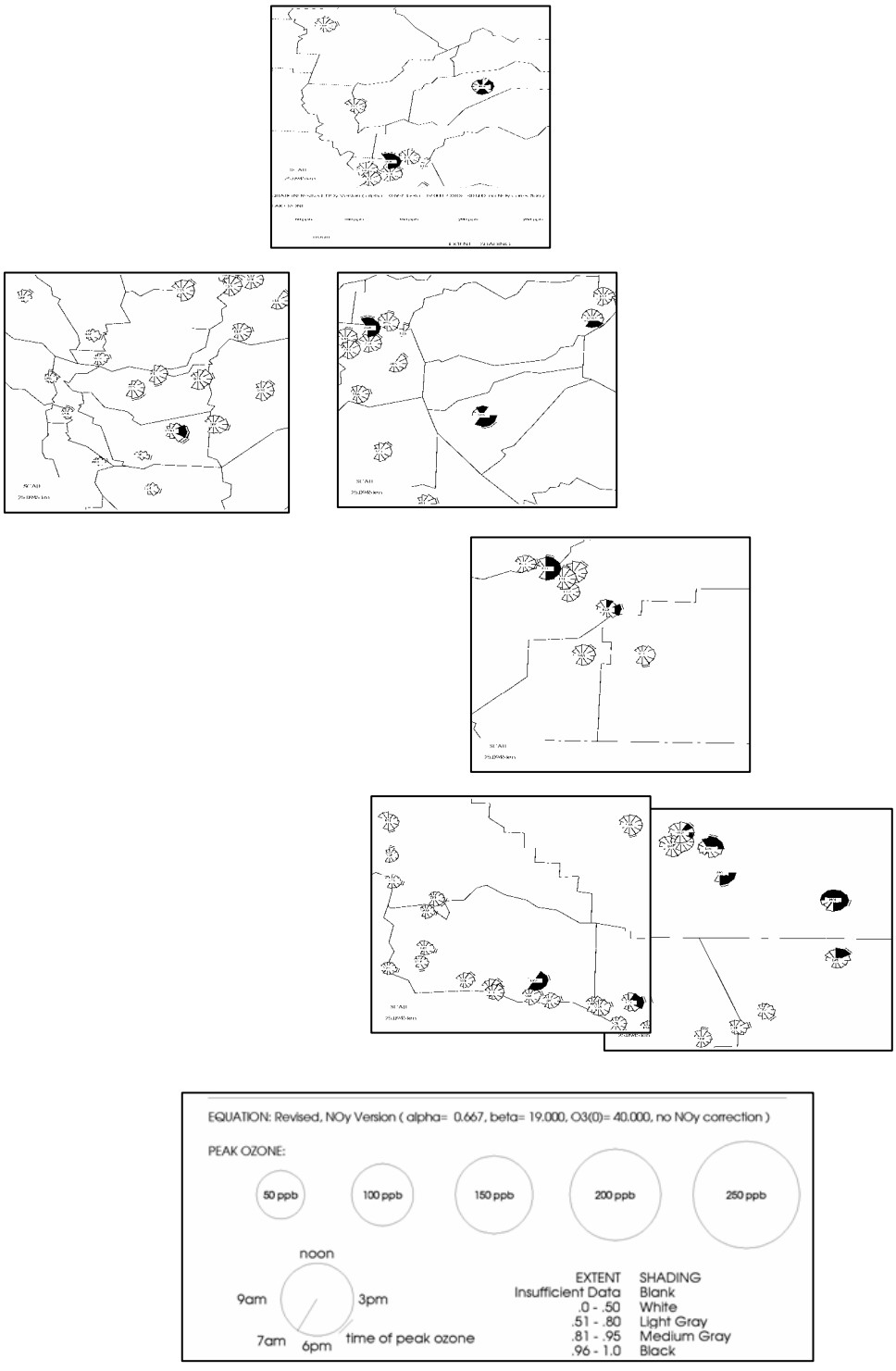

Figure 5-12. Mapper plots showing extent of reaction at selected monitoring sites in the CCOS modeling domain on July 31, 2000 (source: ARB, 2004).

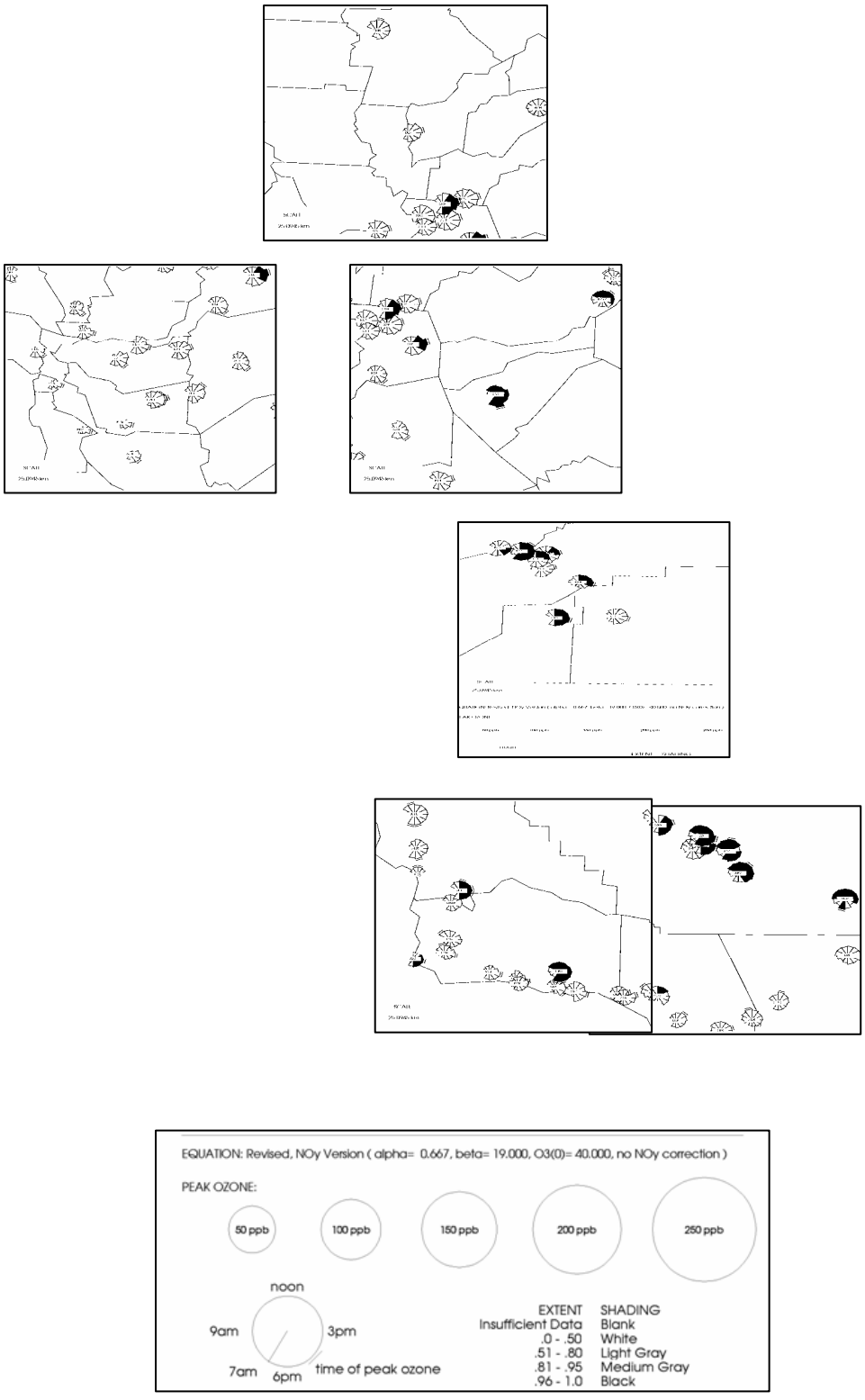

Figure 5-13. Mapper plots showing extent of reaction at selected monitoring sites in the CCOS modeling domain on August 1, 2000 (source: ARB, 2004).

The patterns in simulated ozone concentrations on July 31 and August 1 are similar to those seen on July 30 with some differences as discussed below.

On July 31, 2000, Figure 5-6b shows that the combined NO_x emissions from the Pittsburg and CCPP power plants are transported to the southeast in the base CMAQ simulation. Immediately downwind of the plants, the emitted NO_x scavenges surface ozone, resulting in concentrations that are about 10 ppb lower than the background ozone. In the APT simulation (Figure 5-7b), the PiG treatment of these plants results instead in a plume whose transport is more towards the ESE rather than the SE, with titration of ozone occurring in the former direction. These results suggest that there are some differences in wind direction between the surface layer and layers aloft, so that some of the NO_x emitted from the power plants travels in slightly different directions in the base and APT simulations. Hence, the apparent increases in ozone seen southeast of the plants in the "APT-Base" plot in Figure 5-8b is due to titration of background ozone resulting from different transport directions in the CMAQ simulation rather than any ozone production in the APT simulation.

For isolated NO_x point sources that are located in an environment that is primarily NO_x-limited for O_3 formation, the effect of PiG treatment on O_3 concentrations follows the pattern that was discussed in detail by Karamchandani et al. (2000a) for the Cumberland and Paradise power plants in the Nashville/Tennessee simulation. In the current study, this pattern is exemplified by the Portland Cement plant located in southeastern Kern County because it is fairly well isolated from the other point sources selected for PiG treatment. The plant is near the station MOF in the mapper plot for August 1, 2000 shown in Figure 5-13. This station is NO_x-limited with an "extent of reaction" that is above 0.9 for the majority of hours and between 0.5 and 0.9 for the remainder of the day. The Portland Cement source has a stack height of 45 m.

Figures 5-9a and 5-10a show that, on August 1, the winds are northwesterly near the vicinity of the Portland Cement source, and the plume travels approximately to the southeast. It can be seen from Figure 5-11a that the PiG treatment results in an increment in O_3 concentrations (of about 1 to 4 ppb) near and upwind of the source and decrements

in O_3 concentrations (of about 1 to 4 ppb) from about 10 to 15 km immediately downwind (i.e., southeast of the source) as compared to the base simulation. The near-source increment results from the fact that the PiG treatment prevents the rapid mixing of the plume NO to the surface and, consequently, there is less titration of the existing O_3 by plume NO. Farther downwind, the PiG treatment reduces the formation of O_3 from the point source NO_x emissions by limiting the availability of the plume NO_x. In the base simulation, plume NO_x is rapidly mixed within the grid system and is therefore available for the production of O_3. In the CMAQ-APT simulation, the NO_x emitted from the point source is mixed with the background air according to the rate of the plume dispersion, and O_3 formation is delayed until the plume has become sufficiently diluted. Even farther downwind, the O_3 decrements disappear, and the two simulations give identical results at about 40 km downwind.

Over the three-day period from July 30–August 1, 2000, use of the PiG treatment in the CCOS domain results in ozone production that is up to 10 ppb lower in some areas and up to 6 ppb higher in others than that seen in the corresponding base CMAQ simulation. The maximum decrement occurs in the southeastern part of the domain at a location where the APT O_3 concentration is 46 ppb, 0.5 ppb above the background value of 45.5 ppb and 10 ppb below the base simulation value. The maximum increment of 6 ppb also occurs in the southeast; in this case, the background, base, and APT O_3 concentrations are 55, 59 and 65 ppb, respectively. Larger differences between the APT and base simulations were seen in an earlier PiG study of the NARSTO domain encompassing the eastern United States (EPRI, 2001; Karamchandani et al., 2002). For example, decreases in surface ozone of 37 ppb were seen downwind of the Cumberland plant on applying APT. The impact due to APT is less dramatic in this study since the largest CCOS source selected for PiG treatment emits only about 15 Mg/day of NO_x; emissions from all ten PiG sources total about 101 Mg/day and represent about 4% of the NO_x emissions in the CCOS domain. In contrast, the NO_x emissions from PiG sources in the NARSTO domain ranged from 56 to 457 Mg/day and totaled 5765 Mg/day.

Overall, the total O_3 mass integrated across the CCOS domain over all model layers is slightly higher (by 0.02%) in the APT simulation than in the base simulation. In the

surface layer, the total O_3 mass integrated across the CCOS domain is also slightly higher (by 0.11%) in the APT simulation. These differences are in agreement with those seen in the earlier NARSTO APT study (EPRI, 2001; Karamchandani et al., 2002). There, total O_3 mass was higher in the APT simulation by 0.4% over all layers and by 0.6% in the surface layer.

5.3 Impacts on HNO_3 Concentrations

Figure 5-14 presents the spatial patterns of surface HNO_3 concentrations simulated in the CMAQ base case at 3 p.m. PDT on July 31, 2000 in (a) the entire domain and (b) a small sub-domain covering the extended San Francisco Bay Area. The hour selected corresponds to the time of maximum base case simulated HNO_3 impact due to the ten largest NO_x-emitting plants in the CCOS domain. Simulated surface HNO_3 concentrations range from 1 to 10 ppb in central California. The peak concentration of 10 ppb is simulated near Bakersfield. Surface HNO_3 concentrations of up to 9 ppb are simulated in the extended Bay Area.

Figure 5-15 shows the differences between surface HNO_3 concentrations from the base and background CMAQ simulations at 3 p.m. PDT on July 31, 2000. The maximum HNO_3 produced by the ten plants in the base simulation in the entire CCOS domain is 1.5 ppb, downwind of the Pittsburg and Contra Costa power plants, compared to a background value of 6 ppb (the background HNO_3 concentrations are shown in Figure 5-16). This maximum occurs at a distance of about 11 km southeast of the Contra Costa power plant. The combined Pittsburg-Contra Costa HNO_3 plume is transported to the southeast in the base simulation (Figure 5-15b), in agreement with the ozone plume shown in Figure 5-6b.

The results of using a PiG treatment on HNO_3 concentrations downwind of elevated NO_x sources are generally consistent with our expectations, discussed in Section 5.1. The maximum HNO_3 production in the Pittsburg-Contra Costa plume in the APT simulation is about 0.2 ppb (over background values ranging from 2 to 7 ppb), from 5 to 50 km downwind and to the east and southeast of the sources (see Figure 5-17).

(a)

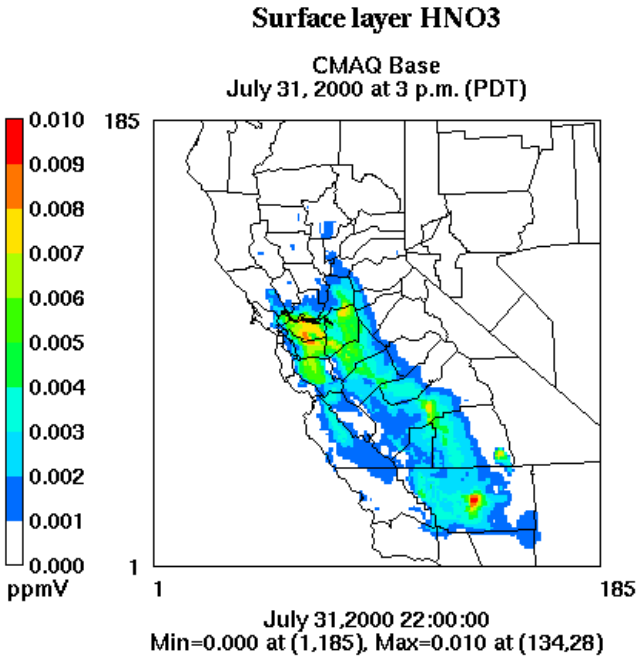

(b)

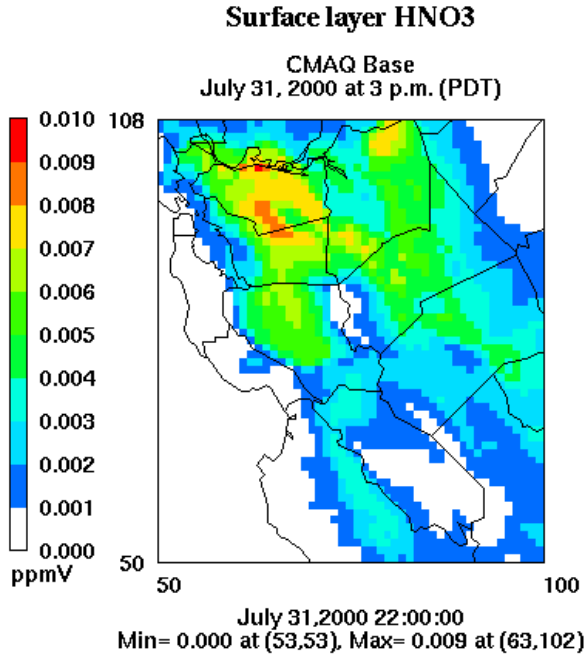

Figure 5-14. Surface HNO_3 concentrations simulated by CMAQ at 3 p.m. PDT on July 31, 2000 in (a) the entire domain and (b) the extended Bay Area.

(a)

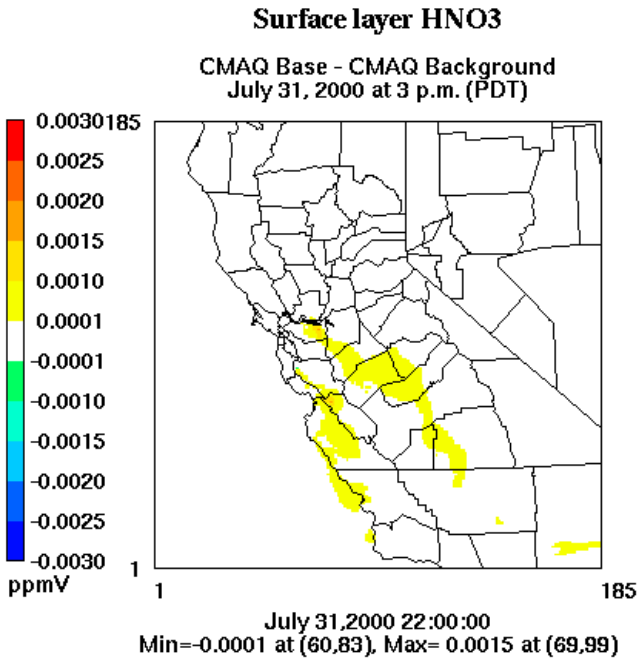

(b)

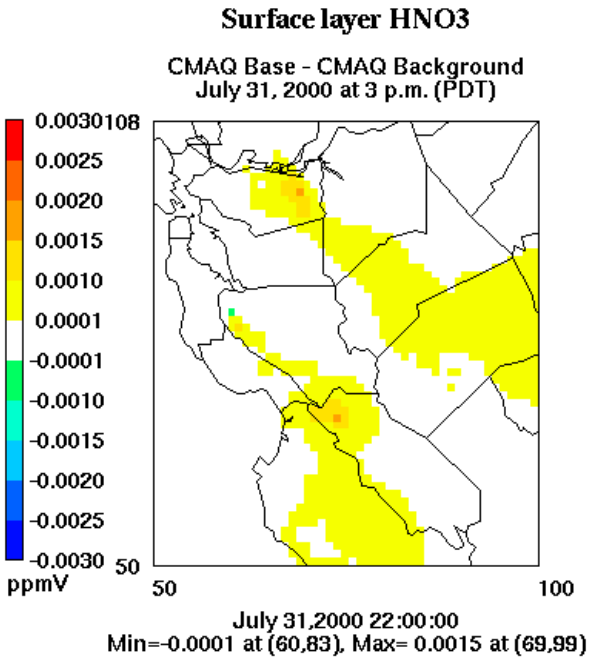

Figure 5-15. Differences (Base – Background) in surface HNO_3 concentrations at 3 p.m. PDT on July 31, 2000 in (a) the entire domain and (b) the extended Bay Area.

(a)

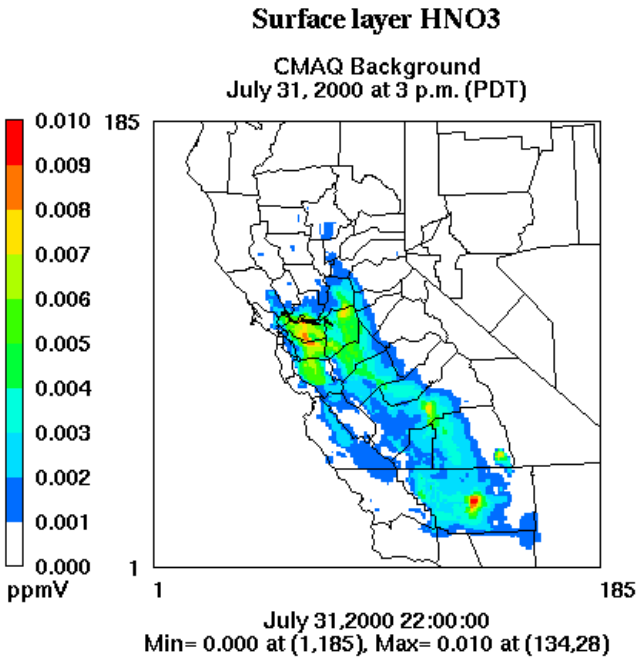

(b)

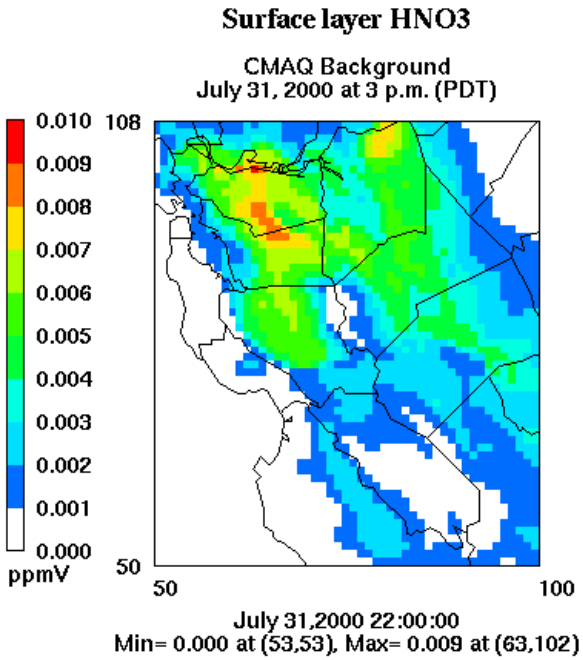

Figure 5-16. Surface HNO_3 concentrations in the background simulation at 3 p.m. PDT on July 31, 2000 in (a) the entire domain and (b) the extended Bay Area.

(a)

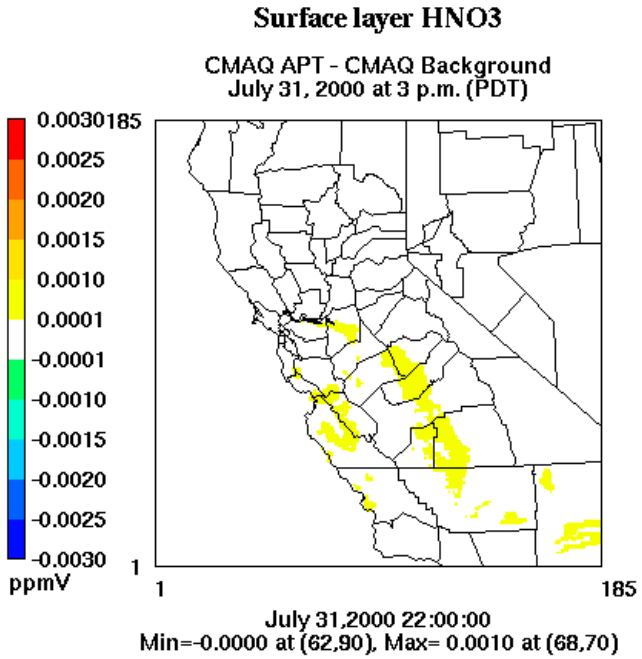

(b)

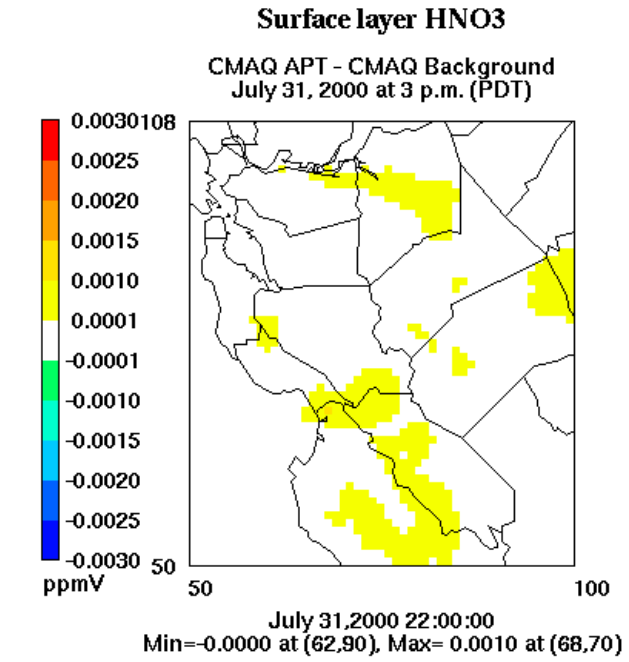

Figure 5-17. Differences (APT – Background) in surface HNO_3 concentrations at 3 p.m. PDT on July 31, 2000 in (a) the entire domain and (b) the extended Bay Area.

The differences in surface HNO_3 concentrations between the base and APT simulations are shown in Figure 5-18. For the combined Pittsburg-Contra Costa plume, the production of HNO_3 in the APT simulation is lower than that in the base simulation. Over most of the areas impacted by the PiG sources in the CCOS domain, the surface HNO_3 concentrations due to the ten plants are about 0.1 to 1 ppb (about 5 to 20%) lower in the APT simulation than in the base case.

The HNO_3 impacts for the Moss Landing plume are somewhat different than those for the Pittsburg-Contra Costa power plant plume. We see from Figure 5-17 that, in the APT simulation, the surface HNO_3 concentration near the source is about 1 ppb over the background value of 0.3 ppb, while the corresponding HNO_3 increment from the base simulation (Figure 5-14) is about 0.4 ppb. Thus, it appears that more HNO_3 is produced in the APT simulation than in the base simulation near the source. This appears to be counter-intuitive based on the expected behavior discussed in Section 5.1. However, an examination of the HNO_3, NO_x and NO_y concentrations at this location shows that the HNO_3/NO_x and HNO_3/NO_y ratios in the APT simulation are about a factor of two lower than those in the base simulation (for example, the HNO_3/NO_y ratio is 0.07 vs. 0.12 for APT vs. Base). In other words, there is slower conversion of the NO_x to HNO_3 in the APT simulation, but this is more than compensated by the higher NO_x concentrations in the APT simulation (18 ppb vs 5 ppb in the base), resulting in higher HNO_3 concentrations near the source as compared to the base case. The surface NO_x concentrations are likely lower in the base case because the emissions are released in several layers and rapidly mixed vertically within the planetary boundary layer. In contrast, the plume model in APT maintains the integrity of the plume material leading to greater NO_x concentrations at the surface. The higher surface NO_x concentrations in the APT simulation are also consistent with the higher titration and consequently lower concentration of ozone (8 ppb less than the base) simulated at this location (see Figure 5-8b).

(a)

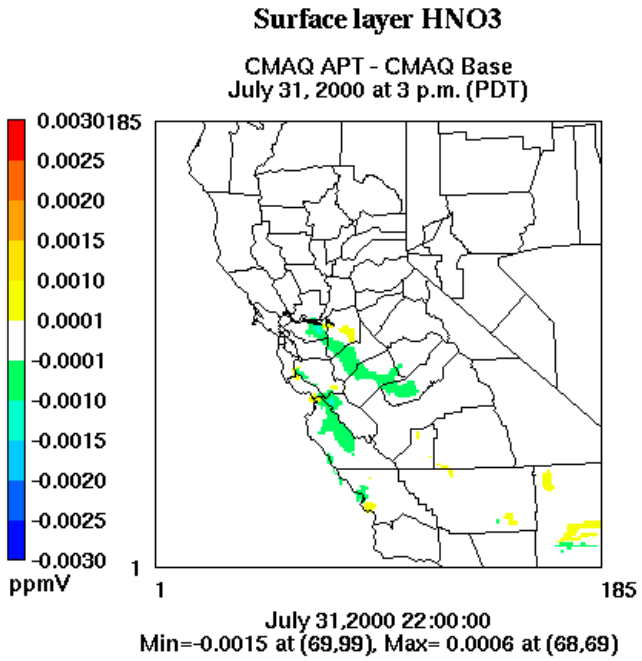

(b)

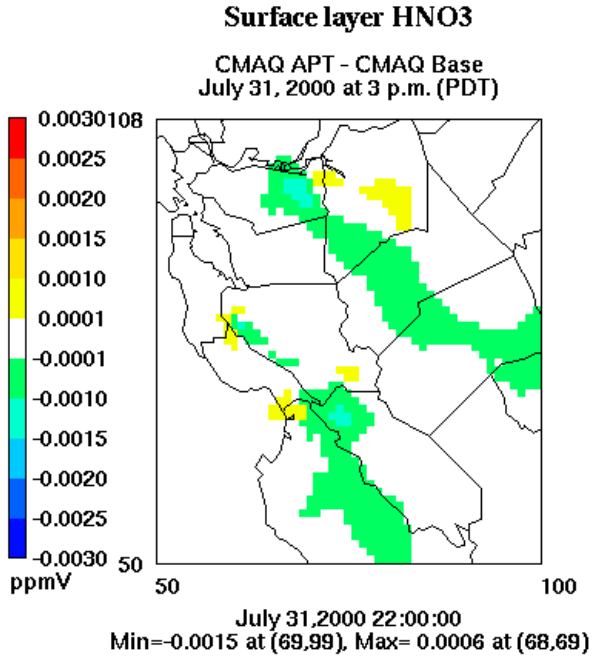

Figure 5-18. Differences (APT – Base) in surface HNO_3 concentrations at 3 p.m. PDT on July 31, 2000 in (a) the entire domain and (b) the extended Bay Area.

The total HNO_3 mass integrated across the CCOS domain over all model layers is lower (0.24%) in the APT simulation than in the base simulation. In the surface layer, the total HNO_3 mass integrated across the CCOS domain is also lower (0.21%) in the APT simulation. The direction of these differences is in agreement with that seen in the earlier NARSTO APT study (EPRI, 2001; Karamchandani et al., 2002). There, total HNO_3 mass was lower in the APT simulation by 10% over all layers and by 5% in the surface layer. The smaller differences seen in the current study are due to the lower levels of NO_x emissions from PiG sources in the CCOS domain than in the NARSTO domain.

6. SUMMARY

Several improvements were made to the plume-in-grid (PiG) model, CMAQ-APT, including the incorporation of an optional treatment for the effects of building downwash in the embedded plume model, SCICHEM, and modifications necessitated by updates in the latest versions of CMAQ (version 4.3 released in September 2003) and SCICHEM (version 1601 released in January 2004). The Young & Boris chemistry solver was also implemented in the current version of CMAQ-APT to retain compatibility between the host and plume models. Test studies showed insignificant differences in ozone and HNO_3 concentrations between simulations using the Young & Boris solver and EBI, the default solver in CMAQ.

CMAQ-APT was applied over the CCOS domain in central California for the four-day ozone episode from 12 GMT on July 29, 2000 to 12 GMT on August 2, 2000. The selection of the modeling period was based on the duration of CAMx emissions and meteorology provided by ARB that were used to create the final CMAQ input files for this study. The ten largest NO_x emitting plants (with a total of 56 stacks) in the CCOS domain were explicitly simulated with PiG treatment. These included the Pittsburg, Moss Landing, and Contra Costa power plants, the Martinez Refinery, and several cement plants and other facilities in central California. A "background" simulation was also conducted in which the emissions from these stacks were neglected. Differences in the results between the background simulation and the base and APT simulations provide a measure of the contribution of these point sources to O_3 and HNO_3 concentrations with and without PiG treatment.

Model performance was evaluated for surface concentrations of ozone, NO_x, NO_y, and CO within the entire domain and in four major sub-regions in central California for the three-day period from 0 PDT on July 30, 2000 to 23 PDT on August 1, 2000. Air quality data provided by ARB were used for the performance evaluation. In general, the performance of CMAQ-APT is comparable to or slightly better than that of CMAQ.

The best performance for 1-hour ozone concentrations for both CMAQ and CMAQ-APT is noted for the Sacramento/Delta area on July 30, 2000. Both models meet EPA's

performance goals for normalized error and unpaired peak prediction accuracy in the four sub-regions on July 30 and 31, 2000. However, neither model meets these goals on August 1, 2000 in any sub-region. Moreover, both models exhibit generally large negative biases, particularly on July 31 and August 1, 2000.

The large underestimates in surface ozone predictions by both models are likely due, in part, to possible errors in the VOC speciation in the emissions inventory and uncertainties in the MM5 meteorology. ARB has reported that the performance of another air quality model, CAMx, was superior when using CALMET/MM5 hybrid meteorology rather than MM5 alone, since the former best utilizes the available CCOS meteorological measurements and takes advantage of the physics in MM5. This hybrid meteorology was not available to us for the study described here.

The simulation results show that the use of CMAQ-APT has an effect on the spatial patterns of O_3 and HNO_3 surface concentrations downwind of the sources considered for PiG treatment up to distances of about 50 to 100 km. O_3 concentrations in the APT simulation show both decrements and increments with respect to the base simulation. The maximum decrement and increment under ozone production conditions are about 10 and 6 ppb, respectively. The maximum decrement occurs in the southeastern part of the domain at a location where the APT O_3 concentration is 46 ppb, 0.5 ppb above the background value of 45.5 ppb and 10 ppb below the base simulation value. The maximum increment of 6 ppb also occurs in the southeast; in this case, the background, base, and APT O_3 concentrations are 55, 59 and 65 ppb, respectively. Significantly larger differences between the APT and base simulations (between 30 and 40 ppb ozone) were seen in the previous CMAQ-APT application over the northeastern United States; however, in that study, NO_x emissions from the largest point sources were one to two orders of magnitude higher than those in the CCOS domain.

A comparison of the base simulation and APT simulation results with those from the background simulation shows that the O_3 decrements are associated with either lower production or greater titration of O_3 downwind of the point sources in the APT simulation relative to the base simulation. The maximum increase in O_3 concentrations in the APT

simulation over the background values (i.e. the maximum ozone production due to the PiG sources) in the CCOS domain is 10 ppb (about 19% of the background) and occurs about 20 km downwind of the Riverside and California cement plants, while in the base simulation, the maximum increase over the background is 11 ppb (about 20%) and occurs about 15 km downwind of the Hanson Permanente cement plant. The plants mentioned above have short stacks (i.e., less than 25 m). For taller stacks such as those at the Pittsburg power plant, ozone production is generally more delayed in the APT simulation than in the base simulation and occurs farther downwind.

The VOC vs. NO_x-limited nature of the background environment, as determined from air quality data in different parts of the CCOS domain during the 2000 July/August ozone episode, was used to understand the differences in ozone production and destruction between the APT and base results. The large increments in O_3 concentrations from the base in the APT simulation are primarily associated with the higher titration of background O_3 in the base simulation near and upwind of the point sources, particularly in VOC-limited environments such as in the San Francisco Bay Area. Here, the effect of the PiG treatment is primarily to limit titration of O_3 by NO. For example, less surface ozone is titrated in the APT simulation than in the base simulation immediately downwind of the Pittsburg and the Contra Costa Power Plants. At a distance of about 60 to 80 km downwind of these plants, there is some production of ozone in the base simulation, while ozone titration continues in the APT simulation. Even farther downwind (about 120 km), where the atmosphere is mostly NO_x-limited, the APT simulation transports more NO_x to those areas than the base simulation, leading to slightly more (up to 1 ppb) ozone production. Thus, increments from the base in the APT simulation are associated with either higher titration of existing O_3 in the base simulation or delayed production of O_3 farther downwind in the APT simulation, as the plume NO_x is transported and exposed to a NO_x-limited environment.

The decrements and increments in ozone compensate each other so that over the entire domain and episode, the difference in the total O_3 mass in the two simulations is negligible (see below). Therefore, the PiG treatment redistributes the O_3 concentrations in a more realistic manner, but does not affect the total O_3 budget significantly. Similar

results were obtained in the previous application of CMAQ-APT to the northeastern United States.

For isolated NO_x point sources that are located in an environment that is primarily NO_x-limited for O_3 formation, such as near the Portland cement plant in the southeastern part of the CCOS domain, the PiG treatment reduces the formation of O_3 from the point source NO_x emissions by limiting the availability of the plume NO_x about 5 to 10 km downwind of the source. Farther downwind, the O_3 decrements disappear, and the two simulations give identical results at about 40 km downwind of the source.

Over the four-day simulation period, the total O_3 mass integrated across the modeling domain over all model layers is slightly higher (by 0.02%) in the APT simulation than in the base simulation. In the surface layer, the total O_3 mass integrated across the modeling domain is also slightly higher (by 0.11%) in the APT simulation than in the base simulation. This is due, in part, to the fact that the generally lower production of O_3 downwind of major NO_x point sources in the APT simulation is more or less compensated by the unrealistically large titration of existing surface O_3 by the NO_x emissions in the base simulation without PiG treatment

Simulated surface HNO_3 concentrations range from 1 to 10 ppb in central California during the July 29-August 1, 2000 period. Differences in surface HNO_3 concentrations in the base, APT, and background simulations were examined at the hour of maximum base case simulated HNO_3 impact due to the ten largest NO_x-emitting plants in the CCOS domain. At this hour, the differences between the APT and base case results range from a maximum decrement of 1.5 ppb in the APT simulation from the base to a maximum increment of 0.6 ppb. The maximum HNO_3 produced due to the top 10 NO_x emitting plants in the base simulation in the entire CCOS domain is 1.5 ppb (compared to a background value of 6 ppb), about 10-15 km downwind of the Pittsburg and Contra Costa power plants. This is significantly higher than the maximum HNO_3 production of about 0.2 ppb in the Pittsburg-Contra Costa plume in the APT simulation. The maximum HNO_3 produced in the APT simulation in the entire CCOS domain is 1 ppb. Over most of the areas impacted by the top 10 NO_x emitting plants, the surface HNO_3 concentrations

in the APT simulation are about 0.1 to 1 ppb (1 to 25%) lower than those in the base simulation.

Over the four-day simulation period and the entire modeling domain, the APT simulation leads to 0.24% less HNO_3 than the base simulation. In the surface layer, the APT simulation leads to 0.21% less HNO_3 than the base simulation. The differences are primarily due to the generally lower production of HNO_3 downwind of the major NO_x point sources in the APT simulation as compared to the base simulation.

The relatively small effect of PiG treatment on the total HNO_3 mass budget is due to the fact that the NO_x emissions from the ten plants treated with PiG amount to only about 4% of the CCOS domain-wide inventory. Larger effects of the PiG treatment on the HNO_3 budget are expected if the sources selected for PiG treatment comprise a larger fraction of the domain-wide NO_x emissions. This has been shown in the application of CMAQ-APT to the northeastern U.S. (Karamchandani et al., 2002) where the HNO_3 budget was about 5 to 10% lower in the APT simulation than in the base.

The effect of PiG treatment on HNO_3 is an important issue for PM nitrate and regional haze modeling studies. Work is ongoing in a separate project to address the effect of power plant plumes on PM formation and regional haze by using a PiG approach for PM in the southeastern United States.

7. REFERENCES

ARB, 2004. http://eos.arb.ca.gov/eos/ARB_Modeling/., California Air Resources Board, Sacramento, CA

Blanchard, C.L. and S. Tanenbaum, 2000. "Spatial mapping of VOC and NO_x-limitation of ozone formation". Report prepared for the Chemical Manufacturers Association, prepared by Envair, Albany, CA.

Blanchard, C.L. and D. Fairley, 2001. Spatial mapping of VOC and NO_x-limitation of ozone formation in central California. *Atmos. Environ*., 35, 3861-3873.

Byun, D.W. and J.K.S. Ching, 1999. Science Algorithms of the EPA Models-3 Community Multiscale Air Quality (CMAQ) Modeling System, EPA-600/R-99/030, U. S. Environmental Protection Agency, Washington, DC.

EPA, 1991. "Guideline for Regulatory Application of the Urban Airshed Model (UAM)", U.S. Environmental Protection Agency, Office of Air Quality Planning and Standards, Research Triangle Park, N.C.

EPA, 1999. "Draft Guidance on the Use of Models and Other Analyses in Attainment Demonstrations for the 8-hr Ozone NAAQS". EPA-454/R-99-004, U.S. Environmental Protection Agency, Office of Air Quality Planning and Standards, Research Triangle Park, N.C.

EPRI, 2001. *Further Development and Evaluation of Models-3/CMAQ-APT.* EPRI Technical Report 1005161, November 2001, Palo Alto, CA.

EPRI, 2003a. Aircraft Measurements of Power Plant Plumes During CCOS and Their Use for the Evaluation of the SCICHEM Model. EPRI Technical Report 1007633, March 2003, Palo Alto, CA.

EPRI, 2003b. Review, Testing and Evaluation of SCICHEM (Second-Order Closure Integrated Puff Model with Chemistry) and CMAQ-APT (Community Multiscale

Air Quality Model – Advanced Plume Treatment). EPRI Technical Report 1005241, 2003, Palo Alto, CA.

Gillani, N.V., 1986. Ozone Formation in Pollutant Plumes: Development and Application of a Reactive Plume Model with Arbitrary Crosswind Resolution, EPA-600/S3-86-051, U.S. Environmental Protection Agency, Research Triangle Park, NC.

Gillani, N.V., J.F. Meagher, R.J. Valente, R.E. Imhoff, R.L. Tanner, and M. Luria, 1998. Relative production of ozone and nitrates in urban and rural power plant plumes 1. Composite results based on data from 10 field measurements days, *J. Geophys. Res.*, **103**, 22,593–22,615.

Gillani, N.V. and J.M. Godowitch, 1999. Plume-in-grid treatment of major point source emissions, Chapter 9, in Byun and Ching, 1999, *op. cit*.

Jackson, B., 2004. private communication, California Air Resources Board, Sacramento, CA.

Karamchandani, P., A. Koo and C. Seigneur, 1998. A reduced gas-phase kinetic mechanism for atmospheric plume chemistry, *Environ. Sci. Technol.*, **32**, 1709–1720.

Karamchandani, P. and C. Seigneur, 1999. Simulation of sulfate and nitrate chemistry in power plant plumes, *J. Air Waste Manage. Assoc.*, **49**, PM-175–181.

Karamchandani, P., K. Vijayaraghavan, S.-Y. Wu, C. Seigneur, L. Santos, I. Sykes, J.-F. Louis, T. Nehrkorn and J. Henderson, 2000a. *Development and Evaluation of a State-of-the-Science Plume-in-Grid Air Quality Model*, Draft Report, EPRI, Palo Alto, CA.

Karamchandani, P., L. Santos, I. Sykes, Y. Zhang, C. Tonne and C. Seigneur, 2000b. Development and evaluation of a state-of-the-science reactive plume model, *Environ. Sci. Technol*., **34**, 870–880.

Karamchandani, P. and K. Vijayaraghavan, 2001. *Planning Studies for Power Plant Plume Measurements During CCOS 2000*, AER Report CP073-01-1, prepared for San Joaquin Valleywide Air Pollution Study Agency, February 2001, Sacramento, CA.

Karamchandani, P., C. Seigneur, K. Vijayaraghavan and S.-Y. Wu, 2002. Development and application of a state-of-the-science plume-in-grid model, *J. Geophys. Res*., 107, 4403-4415.

Kumar, N. and A.G. Russell, 1996. Development of a computationally efficient, reactive subgrid-scale plume model and the impact in the northeastern United States using increasing levels of chemical detail, *J. Geophys. Res.,* **101**, 16,737–16,744.

Lehrman, D., D. Bush, B. Knuth, D. Fairley, and C. Blanchard, 2004. *Characterization of the CCOS 2000 Measurement Period.* Final report under Contract No. 01-2CCOS, prepared for the San Joaquin Valleywide Study Agency and the California Air Resources Board, prepared by Technical & Business Systems, Santa Rosa, CA.

Morris, R.E., M.A. Yocke, T.C. Myers, and R.C. Kessler, 1991. Development and testing of UAM-V: A nested-grid version of the Urban Airshed Model, *Proc. AWMA Specialty Conference: Tropospheric Ozone and the Environment II*.

Myers, T.C., P.D. Guthrie and S.-Y. Wu, 1996. *The Implementation of a Plume-in-Grid Module in the SARMAP Air Quality Model (SAQM)*, SYSAPP-96/06, Systems Applications International, Inc.

Pun, B., J. F. Louis, P. Pai, C. Seigneur, S. Altshuler and G. Franco, 2000. Ozone Formation in the California San Joaquin Valley: A critical assessment of modeling and data needs, *J. Air Waste Manage. Assoc*., **50**, 961-971.

Richards, L.W., J.A. Anderson, D.L. Blumenthal, A. Brandt, J.A. Mcdonald, N. Waters, E.S. Macias and P.S. Bhardwaja, 1981. The chemistry, aerosol physics and

optical properties of a western coal-fired power plant plume, *Atmos. Environ.*, **15**, 2111–2134.

Schulman, L.L., D.G. Strimaitis and J.S. Scire, 2000. Development and evaluation of the PRIME plume rise and building downwash model, *J. Air Waste Manage. Assoc*., **50**, 378-390.

Seigneur, C., T.W. Tesche, P.M. Roth, and M.K. Liu, 1983. On the treatment of point source emissions in urban air quality modeling, *Atmos. Environ.,* **17**, 1655–1676.

Seigneur, C., B. Pun, P. Pai, J. F. Louis, P. Solomon, C. Emery, R. Morris, M. Zahniser, D. Worsnop, P. Koutrakis, W. White and I. Tombach, 2000. Guidance for the performance evaluation of three-dimensional air quality modeling systems for particulate matter and visibility, *J. Air Waste Manage. Assoc*., **50**, 588-599.

Seinfeld, J.H. and S.N. Pandis, 1998. Atmospheric Chemistry and Physics. John Wiley and Sons, Inc., New York.

Sillman, S., J.A. Logan, and S.C. Wofsy, 1990. A regional scale model for ozone in the United States with subgrid representation of urban and power plant plumes, *J. Geophys. Res.,* **95**, 5731–5748.

Sykes, R.I., W.S. Lewellen, S.F. Parker and D.S. Henn, 1988. *A Hierarchy of Dynamic Plume Models Incorporating Uncertainty, Volume 4: Second-order Closure Integrated Puff*, EPRI, EPRI EA-6095 Volume 4, Project 1616-28.

Sykes, R.I., S.F. Parker, D.S. Henn and W.S. Lewellen, 1993. Numerical simulation of ANATEX tracer data using a turbulence closure model for long-range dispersion, *J. Appl. Met.*, **32**, 929–947.

Sykes, R.I. and D.S. Henn, 1995. Representation of velocity gradient effects in a Gaussian puff model, *J. Appl. Met.*, **34**, 2715–2723

Tesche, T.W., D.E. McNally, J.G. Wilkinson, H.E. Jeffries, Y. Kimura, C. Emery, G. Yarwood, 2004. *Evaluation of the 16-20 September 2000 Ozone Episode for use in 1-Hr SIP Development in the California Central Valley,* Report AG-90/TS201, prepared for California Air Resources Board and San Joaquin Valley Unified APCD, February 2004.

Tonnesen, 2003. "Selection of Model for CCOS 2000 SIP Applications", Memorandum to California Air Resources Board, prepared by University of California, Riverside, CA.

U.S. Census Bureau, 1998. http://www.census.gov/geo/www/tiger/index.html.

Young, Y.R. and J.P. Boris, 1977. A numerical technique for solving stiff ordinary differential equations associated with the chemical kinetics of reactive-flow problems. *J. Phys. Chem.*, **81**, 25.